POLITECNICO DI MILANO

Scuola di Ingegneria Industriale e dell'Informazione

Laurea Specialistica in Ingegneria Elettronica
Dipartimento di Elettronica, Informazione e Biomedica

Effects of External Tunable Optical Feedback on Linewidth and Stability of a semiconductor Mode-Locked Laser

Relatore: **Univ.-Prof. Andrea Ivano MELLONI**

Correlatore: **Univ.-Prof. Jeremy WITZENS**

Tesi di Laurea di: **Andrea ZAZZI**
Matricola: 854074

Anno Accademico 2016-2017

Declaration of Authorship

I hereby declare that I have written this master thesis on my own and I have mentioned all the sources and material used correctly, according to the established academic citation rules.

Milano, 2017

Andrea Zazzi

Acknowledgement

"Happyness can be found,
even in the darkest of times,
if one only remembers to
turn on the ***light***."
J.K. Rowling

To Johannes, who guided me through the beautiful and impervious initial *waves*,

To Professor Witzens and the whole IPH Institute who welcomed me and made me feel home,

To Professor Melloni, who supported me even in a different country,

To my family, without whom I wouldn't be here and most of all I wouldn't be me,

To Xhesika and Silvia, architects who have built not only great edifices but also an amazing friendship,

To all my friends, who have always been, through their diversity, source of motivation and inspiration.

And also to you, if you are spending some of your time to read my work,

Thank you.

Abstract

In this thesis we investigate the effects of external tunable optical feedback on the linewidth and stability of a semiconductor mode-locked laser, through a silicon photonic integrated circuit. We aim to find a stabilization method which exploits tuning of feedback amplitude and phase to reduce the linewidth of the lines of the comb, i.e. reducing phase noise which affects the stability of the laser. A detailed characterization of every photonic devices integrated in the PIC is presented and an experimental analysis of feedback regimes is shown. In particular, the positive effects of filtered feedback when the laser operates in a bad mode-locking condition is shown, when two neighbor lines of the comb are separately filtered in two feedback branches and reflected back to the laser, reaching a reduction of both optical and RF linewidth.

Sommario

Lo scopo di questa tesi e' quello di analizzare l'effetto del feedback ottico esterno, applicato attraverso un circuito fotonico integrato, sulla larghezza di riga a sulla stabilita' di un laser mode-locked a semiconduttore. L'obiettivo e' trovare un metodo di stabilizzazione che sfrutti il regolamento dell'ampiezza e della fase del feedback per ridurre la larghezza delle linee dello spettro a pettine del laser, cioe' ridurre il rumore di fase che ne inficia la stabilita'. Ogni dispositivo fotonico integrato nel PIC viene caratterizzato e i regimi del feedback sono analizzati sperimentalmente. In particolare vengono messi in risalto gli effetti positivi del feedback quando il laser opera in una condizione di mode-locking non ottima, filtrando separatamente due linee vicine dello spettro, grazie ai risonatori ad anello, nei due bracci del feedback che, dopo essere state riflesse, causano una riduzione della larghezza di linea sia ottica che RF.

Contents

Declaration of Authorship i
Acknowledgement ii
Abstract v
Contents vi

Table of Pictures **1**

1 Introduction **5**
1.1 Context and Motivations 5
1.2 Applications 6
1.3 State of the Art 7
1.4 Summary of main Achievements 9

2 Laser Theory **11**
2.1 Quantum Dash Lasers 11
2.2 Mode-Locked Laser 14
2.3 Rate Equations 16
2.4 Noise in MLL 18

3 Optical Feedback and Stability Parameters **22**
3.1 Lang Kobayashi Equations 24
3.2 Figures of Interest 26
3.2.1 Optical Linewidth 26
3.2.2 RF Linewidth 26
3.2.3 RF and Optical Linewidth relation 28

4 Setup and PIC Description **31**
4.1 Structure 31
4.2 Laser 35

4.3 Coupling 38
4.4 Photonic Devices 39
4.4.1 Ring Resonators 39
4.4.2 Phase Shifter 43
4.4.3 Sagnac Loop 45
4.4.4 Grating Couplers 46

5 Experimental Results **48**
5.1 Devices Characterizations 48
5.1.1 Ring Resonators Characterization 48
5.1.2 Phase Shifters Characterization 51
5.2 Analysis with Mode-Locked Laser 53
5.2.1 Laser Spectrum Alignement 53
5.2.2 2D Rings Heater Current Scan 54
5.2.3 2D Scan changing the Laser bias current 57
5.2.4 Rings and Phases Current Scans 59

6 Conclusions and Outlook for the Future **64**

Bibliography **67**

Table of Figures

Figure 2.1: Energy levels shape in different nanostructures. Redrawn from *Quantum Dots Solar Cells*, J. E. Khalil

Figure 2.2: Quantum dots energy levels. Redrawn from *Quantum Dots*, Sigma-Aldrich

Figure 2.3: Fabry-Perot cavity structure and mode-locked laser spectrum

Figure 2.3: Laser Band Diagram

Figure 2.4: Active mode-locking. Redrawn from *Active Mode Locking*, RP Photonics

Figure 2.5: Passive mode-locking. Redrawn from *Passive Mode Locking*, RP Photonics

Figure 3.1: Optical feedback regimes. Redrawn from *The Diagram of Feedback Regimes revisited*, S. Donati, R.H. Horng, IEEE Journal of selected topics in Quantum Electronics, Vol. 19, No. 4, July/August 2013

Figure 3.2: Parabolic dependance of optical linewidth. Redrawn from *Optical linewidth of a passively mode-locked semiconductor laser*, N. Rebrova, G. Huyet, S. P. Hegarty, Optics Letters, November 2009, DOI: 10.1364/OL.34.003307

Figure 4.1: Experimental Setup Picture.

Figure 4.2: Photonic Integrated Circuit Layout.

Figure 4.3: Laser Spectrum at different bias currents.

Figure 4.4: Laser Optical Linewidth at different bias currents.

Figure 4.5: Optical Spectrum of the free-running mode-locked Laser.

Figure 4.6: RF Spectrum of the free-running laser at different currents and RF Linewidth for each current, computed through Lorentzian Fit.

Figure 4.7: Gaussian Beam approximation and Inverse Tapered Edge Coupler.

Figure 4.8: All-pass and Add-drop Ring Resonators.

Figure 4.9: Ring Resonators Thermal Heater and Electrical Contacts.

Figure 4.10: Sagnac-Loop structure.

Figure 4.11: Grating Coupler structure.

Figure 5.1: Ring Resonator Characterization.

Figure 5.2: Ring Resonator Transfer Function.

Figure 5.3: Phase Tuner Characterization.

Figure 5.4: Laser Spectrum Alignement to Ring Transfer Function.

Figure 5.5: 2D Scan of ring resonators heater current.

Figure 5.6: Higher resolution 2D Scan in an interesting region.

Figure 5.7: Comparision between Lorentzian Fit and Lorentzian with a top flat plateau to model noise.

Figure 5.8: New Fit Plots.

Figure 5.9: Optical and RF parameters of the Laser changing the oper-

ating point.

Figure 5.10: New 2D Scan after changing Laser operating point.

Figure 5.11: Optical Spectrum and Optical Linewidth of the comb laser under feedback.

Figure 5.12: RF Liniewidth and Optical Power with phase shifters at 0mA.

Figure 5.13: RF Liniewidth and Optical Power with phase shifters at 10mA.

Figure 5.14: RF Liniewidth and Optical Power with phase shifters at 20mA.

Figure 5.15: RF Liniewidth and Optical Power with phase shifters at 30mA.

Chapter 1

Introduction

1.1 Context and Motivations

Feedback can be extremely useful in different systems, because it allows to take one output and route it back with some processing to the system input, making the two signals interacting, stabilizing the operation condition and reducing the output fluctuations. The general goal of a negative feedback structure, whichever the nature of the system, is to reach a stable point of operation with better properties with respect to the open loop structure, or in other words reach an equilibrium point.

In our case, we study the effects of external tunable optical feedback on a mode-locked laser, making the emitted light interacting with itself in a constructive interference condition. In particular we focus on keeping the mode-locking condition of the laser and try to improve it, analyzing the RF linewidth, i.e. the spread of the beating tone of our comb lines, which is a clear indicator of the quality of the locking condition. As we will se in next chapters, both linewidth narrowing and broadening have been reported under optical feedback influence. In an optical system we will have almost always spurious reflections from optical components or Reyleigh backcattering from optical fibers and these can be source of unwanted optical feedback which may cause instability. However, a stable line-narrowing effect can be

mantained controlling precisely the phase and the amplitude of the reflected field. The optical feedback loop exploits different integrated photonic devices such as ring resonators, phase tuners and sagnac loop reflectors to take the laser emitted signal, filter it and shift it in phase and feed it back to the laser source in such a way to have constructive interference between the original signal and the feedback signal, leading to an enhancement of the coherence of our light source.
We decided to implement a controllable external optical feedback exactly to reach this purpose, acting on phase and amplitude of the reflected light to obtain high spectral purity and long-term stability of our comb signal, reducing phase noise and frequency flicker noise effects.

1.2 Applications

An ultra short and stable pulses source can be useful for applications such as multi-channel telecommunications, spectroscopy, metrology and on-chip clock distribution, and noise suppression and frequency stability are crucial for development in these fields. Between all the possible applications, metrology covers a really important role, since the availablility of high speed, high precision and long dynamic measurements is fundamental for science and society development. The advent of optical comb has opened numerous break through possibilities thanks to its interesting features, such as inter-mode interference, high coherence and phase locking between the lines and wide spectral band.
A frequency comb, in fact, can be used as an optical clockwork. Knowing exactly the frequencies of the comb, we can measure unknown frequencies by measuring the beat notes, which describe the difference in frequency between the unknown and the comb frequencies. To perform this in a wide frequency range, of course a comb with a large overall bandwidth is required. It can be used to measure absolute optical frequencies, for example in the microwave domain, but also ratios of optical frequencies, with extremely high precision. In the 90's a new technique based on frequency combs from mode-locked lasers revolutionized optical frequency metrology. This is based on

the comb-shaped spectrum of a mode-locked laser, where the lines are all exactly equidistant, disregarding noise influences, meaning that the comb is determined by two parameters: frequency spacing, or pulse repetition rate, and the absolute position, or carrier-envelope offset. Relating these two parameters to a microwave reference, all optical frequencies can be known and therefore any optical frequency within the range of the comb can be measured with the beating tone. This technique is quite simple and makes possible to construct compact frequency reference sources and frequency measurement devices with a wide spectral range and with a relative low cost.

Optical combs are extremely important also in dimensional metrology, mainly thanks to inter-mode interference, wide spectral bandwidth an long coherence length. A mode-locked laser can be used also to determine distances by measuring the travel time of a pulse based on the speed of light in the air. Using a the pulse train the timing resolution is expected to be enhanced due to short pulse duration and high peak power. Even though the pulses are broadened and chirped while propagating in the air, due to dispersion effects, we can enhance the precision by cross-correlating with pulse-to-pulse interference and since the comb has an high coherence, this will result in an enhancement of precision, which can achieve sub-μm precision over a 700m distance with high reproducibility.[1]

1.3 State of the Art

State of the art frequency oscillator based on single frequency used in metrology rely on frequency multiplication chain, where an oscillator of precise known frequency is used together with a non linear element to generate harmonics of its frequency. A suitable harmonic is than compared with the unknown frequency, measuring the beating tone of the latter with the nearest harmonic. This continues in a step-wise fashion until the desired frequency is reached. As understandable this process is quite complex and expensive and it can cover only discrete frequency in the optical spectrum.
To overcome these problems, optical clocks are used. An optical clock is

basically a clock signal in the radio frequency domain which is generated by a stable comb signal, which guarantees better properties. A wide band comb transfers the stability of the highest quality optical frequency across other optical spectral regions guaranteeing better stability and reproducibility.[2]

It is then fundamental to improve the properties of mode-locked laser, reducing the noise and increasing the phase correlation of the comb lines. External optical feedback, has been demonstrated powerful in this sense, since it was used as stabilization method exploiting coherent interference to reduce optical and RF linewidth and reaching higher coherence in the comb.[3]
Even more interesting is implementing a tunable filtered optical feedback on an integrated circuit based on ring resonators that has been already demonstrated beneficial in terms of laser stabilization against moderate parassitic reflections occurring elsewhere on the chip.[4]

Given these promising results, we aim to use an integrated circuit provided with ring resonators, phase tuners and reflectors, to implement an external tunable optical feedback, where we can control very precisely the feedback parameters, in terms of strength and phase. Tuning them we aim to reach a better stability of our comb laser reducing noise.

1.4 Summary of main Achievements

Here a list of personal achievements and contributions on the topic:

- Build a set-up implementing a new external tunable optical feedback structure with ring resonators and phase shifters, to act independently on phase and amplitude of the feedback field.
- Experimental results showing the beneficial effect of such feedback structure in terms of linewidth reduction of the whole comb, given by the interference between the initial comb and the lines filtered and fed-back by the feedback branches.
- Demonstration of phase noise reduction thanks to feedback, implementing a fitting of RF spectrum through a function which models independently phase noise and frequency fluctuations.
- Experimental results useful as starting point for new investigations on the topic of tunable optical feedback, where the phase effect should be investigated more, always in a joined condition with the ring resonators.

This thesis is structured as follows: in Chapter 2 mode-locked lasers theory useful for the investigation is discussed, in Chapter 3 optical feedback theory and the figures of interests analyzed in this thesis are presented. In Chapter 4 the setup and the photonics chip used are described in detail, while in Chapter 5 experimental results are discussed and the final achievements stated.

Chapter 2

Laser Theory

2.1 Quantum Dash Lasers

Compact dimensions, enhanced performance and reduced costs are fundamental constraints in integrated systems, for this reasons semiconductor nanostrucures are particularly interesting. Semiconductor nanostructures are self-assembled structures in a semiconductor material which can assume different shapes, such as wells, wires and dots, where electrons are quantum confined in different dimensions according to the shape. It's important to analyze the density of electronic states, DOS, of these structures to define the energy levels and the emission spectrum of a system made of multiple nanostructures. The electronic energy quantization is, in fact, primarily determined by the spatial confinement of electrons, given by the nanostructure shape.[5]

The advantage of nanostructures is the possibility to control the properties of material by geometric parameters, like the dot size, without changing the material composition. This allows to combine material properties to reach better results. Quantum dots structures have positive characteristics such as low threshold current, low chirp and small linewidth enhancement factor and quantum dash have similar properties. Quantum dash structures are wire-like semiconductor nanostructures which self-assemble during growth

process. Even though the mechanism is still not completely understood, lasers made of quantum dash material present low threshold current, broad gain spectrum and high wavelength stability.[6]

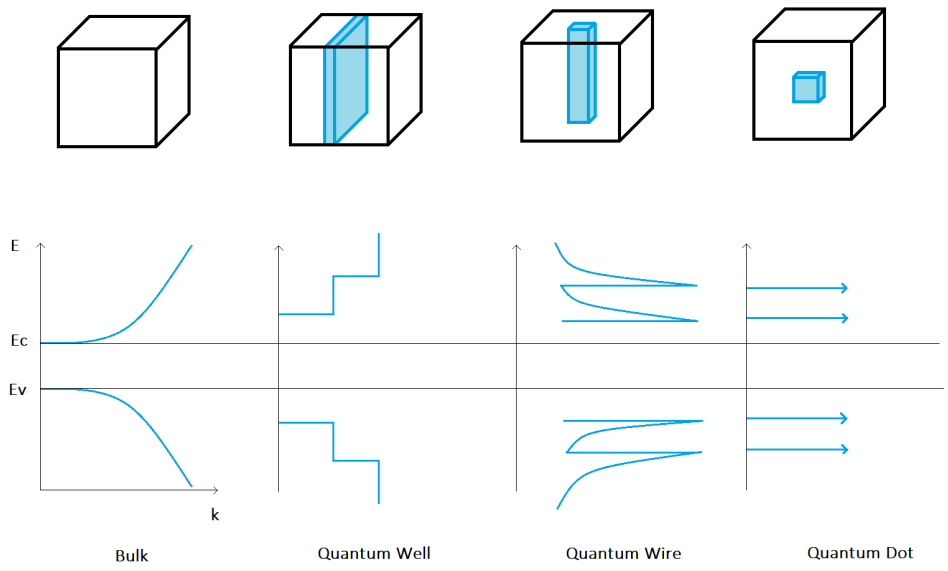

Figure 2.1: Energy levels shape according to different nanostructures. In order, three dimensional bulk structure, two dimensional quantum well structure, one dimensional quantum wire structure and zero dimensional quantum dot structure, where electrons are confined in all the three dimensions.

As we can see in figure 2.1, electrons in nanostructures are confined in a smaller space with respect to a bulk structures and therefore the energy levels are quantized. When the number of atoms in the lattice is reduced, the density of states becomes discrete and the band structure becomes a levels structure. This means that after exciting the material, when it will return to the original state, light will be emitted in a narrower spectrum since energy level are much more defined.

We can extend the quantum dot theory also to quantum dash structures, since it has been observed that they present a similar electronic behavior. As we can see in Figure 2.2, electrons, in a quantum dot structure, are con-

fined in a small space and therefore the energy levels are quantized. As the dot size decreases, the energy gap between valence and conduction levels increases, meaning that more energy is needed to excite the dot and consequently, more energy will be released when the crystal returns to its original state. The main consequence is that quantum dots material can emit any frequency in the allowed spectrum based on the dots size. We have than an emission spectrum depending on a geometric parameter, which we can manipulate quite easily during fabrication processes.[7]

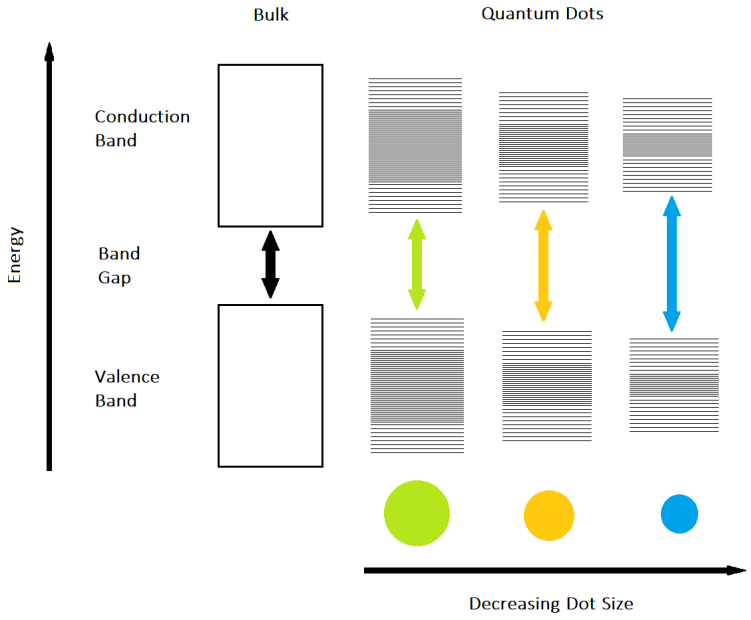

Figure 2.2: Energy levels splitting in quantum dots nanostructure due to quantum confinement effect. The band gap increases when the size of the nanocrystal decreases. QD materials work as broadband since there are many statistical sized dots, which allow emission in a broad spectrum.

2.2 Mode-Locked Laser

Mode locking consists in producing a train of light pulses with really short duration. Considering the laser optical cavity made of two mirrors and a gain medium, the only spectral modes that can be lased are the ones inside the gain bandwidth and that constructively interfere in the cavity, i.e. the frequencies that satisfy the relation $f = 2\pi n \frac{c}{2L}$, where L is the length of the cavity. It is obvious that in this way we will have a separation between different frequencies constant and locked at $\Delta\nu = \frac{c}{2L}$. In a simple laser these frequencies oscillate independently without correlation between their phases, but, if the phase between different modes is fixed, these will all periodically constructively interfere, producing a strong peak of light. The separation of these pulses in time will be $\tau = \frac{2L}{c}$.

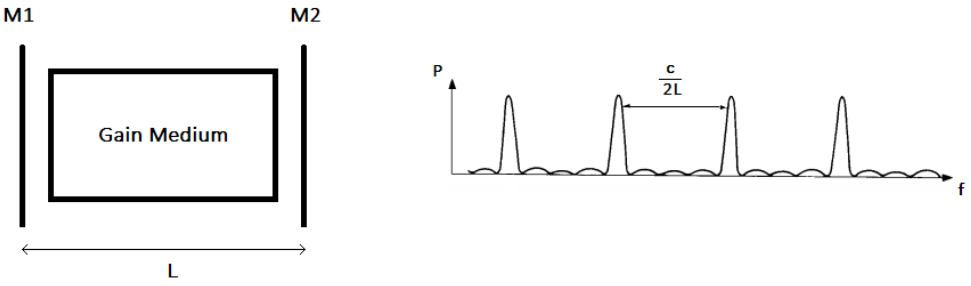

Figure 2.3: Laser Cavity and Spectrum.

We can also describe the output electric field as a comb function, considering the amplitude of each pulse constant

$$E(t) = A \sum_{n=0}^{N-1} e^{i(\omega_n t + \delta_n)} \tag{2.1}$$

where ω_n is the angular frequency of the n^{th} mode and δ_n its relative phase.

It's clear that a comb in frequency, due to multiple frequency modes lased, has a comb shape also in time domain, given the Fourier transform properties.

Mode-locked lasers result particularly interesting in telecommunication and timing application, thanks to the comb shaped emission and extremely short time duration of each pulse. These characteristics, in fact, make the laser more tolerant to dispersion in fibers. They can also be used in Wavelength Division Multiplexing systems since they are a multi-wavelength source, and also as fast oscillators.[8]

We can classify the methods to obtain a mode-locked laser in active or passive. Active methods use an external signal, usually RF, to induce the modulation of the intracavity light, modulating the resonator losses or the round trip phase change. If the modulation is synchronized with the resonator round trip, a pulse with the correct timing can pass the modulator at times where the losses are at minimum, while all the others will be a lot attenuated, and they won't be able to pass.[9]

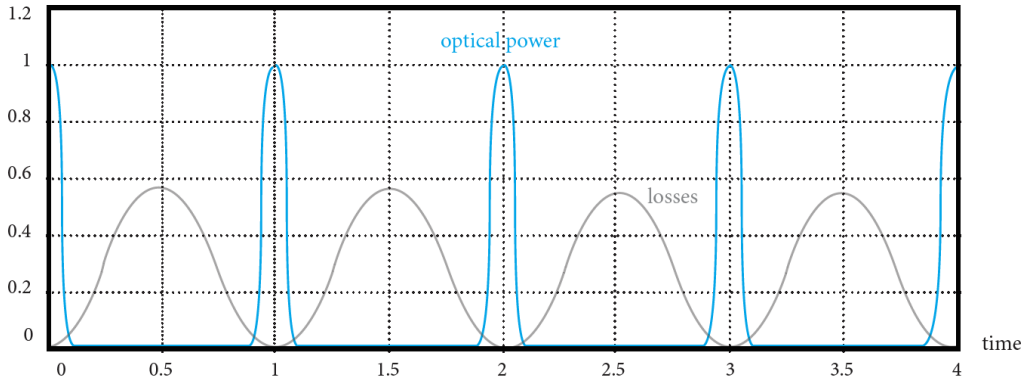

Figure 2.4: Active mode-locking method.

Passive methods, instead, relay on non-linear materials with a saturable absorber, which causes self-modulation of the light. This allows to have pulses much shorter in time, in the order of femtoseconds, thanks to the saturable absorber that can modulate the resonator losses faster than an electronic

modulator. The saturable absorber is, in fact an optical component whose losses depend on optical intensity. For example, in a medium with absorbing dopant ions, a strong optical intensity can lead to the deplation of the ground state of those ions, leading to lower losses. Since we have anyway losses modulation, only the pulses synchronized with the minimum losses will be able to pass, while the others will be almost completely absorbed, leading to the mode-locking condition.[10]

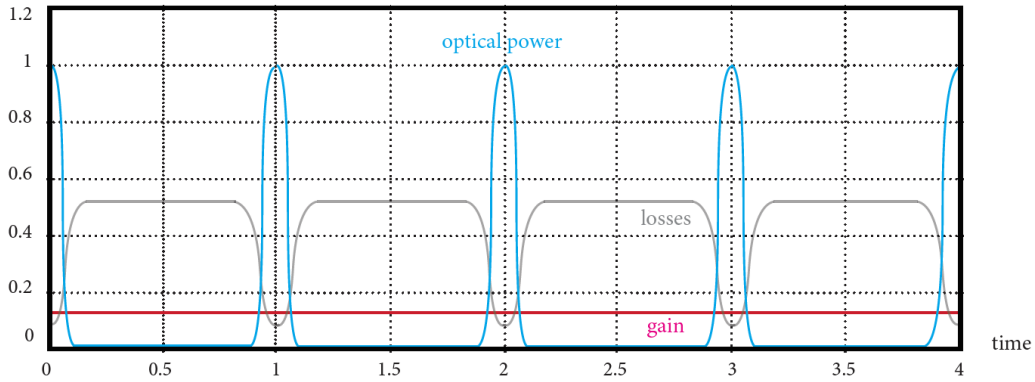

Figure 2.5: Passive mode-locking method.

2.3 Rate Equations

Electrical and optical performances of a laser can be modelled using the well known rate equations, a set of differential equations that relate the photon density and charge carriers to the injection current and material parameters such as carrier and photon life time and optical gain.

If we consider a three energy level system, we can write

$$\begin{aligned}
\frac{\delta n_3}{\delta t} &= -A_{32}n_3 - A_{31}n_3 + \frac{\sigma_{13}I_p}{h\nu_p}n_1 - \frac{\sigma_{31}I_p}{h\nu_p}n_3 \\
\frac{\delta n_2}{\delta t} &= -A_{21}n_2 + A_{32}n_3 + \frac{\sigma_{12}I_s}{h\nu_s}n_1 - \frac{\sigma_{21}I_s}{h\nu_s}n_2 \\
\frac{\delta n_1}{\delta t} &= +A_{21}n_2 + A_{31}n_3 - \frac{\sigma_{13}I_p}{h\nu_p}n_1 + \frac{\sigma_{31}I_p}{h\nu_p}n_3 - \frac{\sigma_{12}I_s}{h\nu_s}n_1 + \frac{\sigma_{21}I_s}{h\nu_s}n_2
\end{aligned} \tag{2.2}$$

where n_j indicates the fractional level population of level j in a way that $n_1 + n_2 + n_3 = 1$. A_{ij} are the spontaneous transition coefficients between level i and level j, while the stimulated emission rates are given by transition cross section σ_{ij}, optical intensity and and photon energy at the pump wavelength p and at the signal wavelength s.

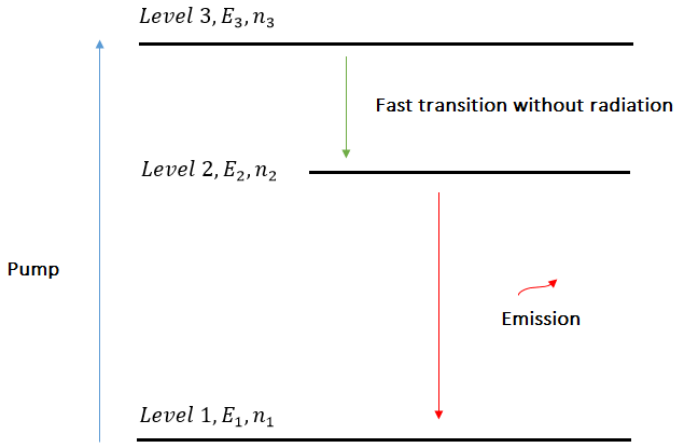

Figure 2.6: Band Diagram.

We can also use a set of equations to describe the field behavior in terms of field amplitude and phase, related of course to the carrier density. Considering the electric field as $E(t) = A(t)e^{-i\phi(t)}$, we can write

$$\begin{aligned} \frac{\delta A(t)}{\delta t} &= \frac{1}{2} G_n [n(t) - n_{th}] A(t) \\ \frac{\delta \phi(t)}{\delta t} &= \frac{1}{2} \alpha G_n [n(t) - n_{th}] \\ \frac{\delta n(t)}{\delta t} &= \frac{J}{ed} - \frac{n(t)}{\tau_s} - G_n [n(t) - n_0] A^2(t) \end{aligned} \tag{2.3}$$

where G_n is the laser gain, n_{th} the threshold carrier density, α the linewidth enhancement factor, J the injection current density, d the active region width, τ_s the carrier life time and n_0 the carrier density at transparence.[11]

2.4 Noise in MLL

The repetition rate of the lines and the strong phase correlation between the optical modes are the main parameters for the quality of a mode-locked laser, so frequency stability and phase noise spectral density have a fundamental role in defining the laser performances. In particular, we can analyze short term and long term frequency stability.[12]

In short term **timing jitter** amplified spontaneous emission represents one of the main sources. ASE noise is generated by photons spontaneously emitted by the intrinsic recombination of electrons and holes in a semiconductor, they are anyway amplified by the cavity leading to phase and intensity fluctuations. Amplified spontaneous emission influences the timing of the pulses and will lead to a broadening of the emission spectrum, that will assume a lorentzian shape. It is clear that to enhance the stability of our laser, we need to reduce this unwanted phenomenon.

Regarding long term **timing drift**, frequency fluctuations of the source affect the emission spectrum. This can take place due to drift in temperature and

environmental noise, that will lead to a drift in frequency, compromising the stability of our laser. For this reason is fundamental to implement a temperature controller to limit temperature drift at the minimum possible. In our set up, both the laser and the chip are connected to a TEC which guarantees a good thermal stability over long time measurements. Both these effects can be easily seen analyzing the RF spectrum of our mode-locked laser, i.e. measuring the beating tone between different lines of the comb. As expected, the spectrum presents a lorentzian shape, but we can estimate independently the two sources of noise fitting the measurements with a function that implement a lorentzian for the flanks but also a flat plateau on top of it, as we can see in figure in the next page, modelling independently white frequency noise, that gives the flanks lorentzian lineshape, and frequency flicker noise, that gives a broadening in the peak.

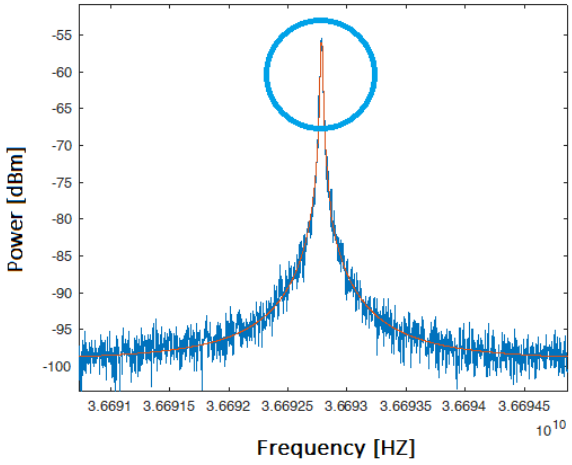

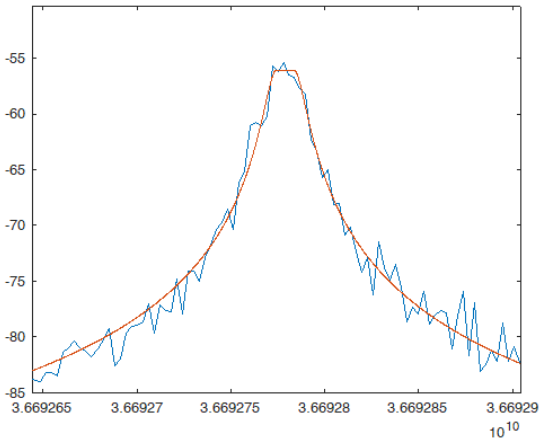

Fitting Function

$$\begin{cases} 10log_{10}\left[\dfrac{p1}{\left(\frac{x-\left(p2-\frac{p5}{2}\right)}{p3}\right)^2+1}+p4\right] & x < p2-\frac{p5}{2} \\ 10log_{10}[p1+p4] & p2-\frac{p5}{2} < x < p2+\frac{p5}{2} \\ 10log_{10}\left[\dfrac{p1}{\left(\frac{x-\left(p2+\frac{p5}{2}\right)}{p3}\right)^2+1}+p4\right] & x > p2+\frac{p5}{2} \end{cases}$$

Fitting Parameters [2.4596e-06, 3.6693e+10, 5.7678e+03, 1.1629e-10, 9.8966e+03]

Chapter 3

Optical Feedback and Stability Parameters

Optical feedback effects depend on the amplitude and phase of the back reflected light, which can lead both to constructive or constructive interference. It is then important to be able to control these parameters and for this reason we implemented and external tunable optical feedback.
To describe and classify the effects of external optical feedback, for a single mode laser, we can use the Tkach and Chraplyvy diagram, shown in Figure 3.1, in which five different regimes can be distinguished.[13] The parameters that define this classification are feedback power ratio, distance to reflection and phase of the incoming power.

In regime 1 we can find stability, the optical linewidth is broadened or narrowed based on the distance to the reflector, which determines the phase of the optical feedback signal.
Regime 2 is characterized by conditional stability, changes in the phase of the feedback signal may cause mode hopping of the laser spectrum, corresponding to external cavity modes between laser output facet and feedback reflector.

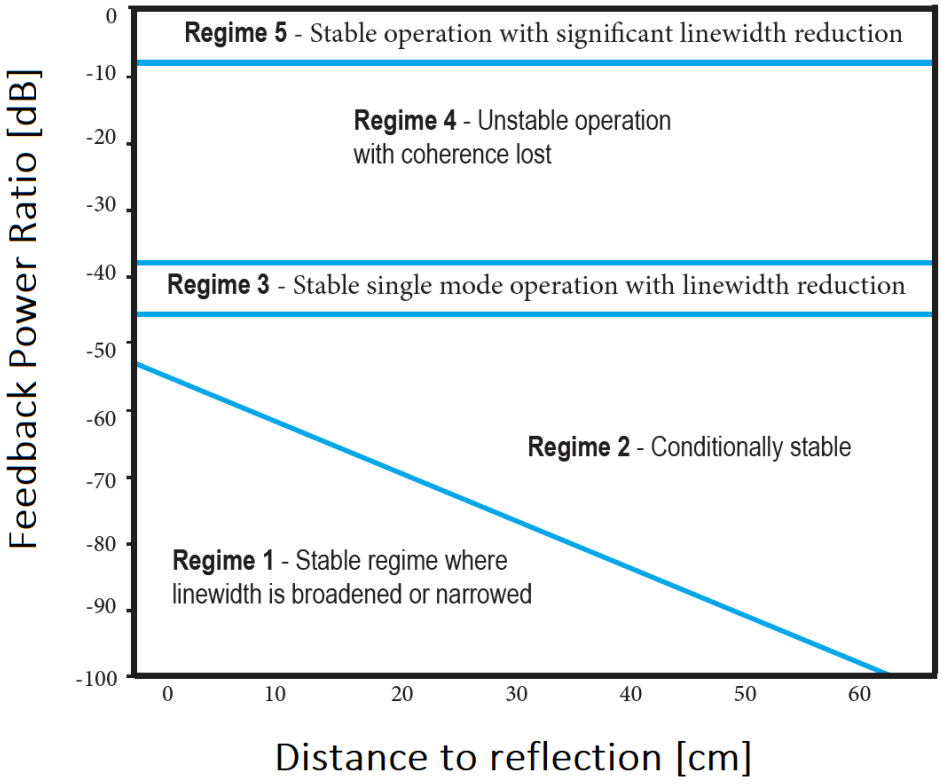

Figure 3.1: Optical feedback regimes classification.

In regime 3, we can see a stable single mode operation with optical linewidth reduction, caused by the very narrow feedback regime.
Regime 4 is characterized by unstable operation with coherence collapse because the laser develops side modes separated from the main mode by the relaxation oscillation frequency.
In regime 5 we have again stable operation conditions with significant linewidth reduction, this usually requires anti-reflection coating on the laser output facet. In this regime the laser is a short active section in a long cavity laser.

Our very last goal is to exploit optical feedback to obtain a stable mode-locked laser and improve its figures of interest, like optical and RF linewidth,

but, since we are using a mode-locked laser, we need to adapt this classification to our needs.
It' possible to define a classification of external optical feedback regimes for mode-locked laser, where the dynamics differ qualitatively from single mode lasers.[14] Once again the effect is classified based on the feedback strength, but also taking into account the ratio between external cavity length L_{ext} and the length of the laser L_{las}, which basically expresses the feedback phase.

We have a first *non resonant case*, when $\frac{L_{ext}}{L_{las}}$ is irrational, i.e. when the reflector has a random position. In this case if the feedback strength is small, we will observe a weaker train of pulses alongside the dominant mode of our mode-locked laser. Instead, if the feedback is strong, we will experience instabilities due to the excitation of a second supermode which competes with the original one.
A second regime can be defined as *fractional resonant case*, when $\frac{L_{ext}}{L_{las}} = \frac{M_1}{M_2}$ with M_1 and M_2 integers. In this case, with strong feedback, a stable regime is possible.
Finally the *integer resonant regime* takes place when $\frac{L_{ext}}{L_{las}}$ is an integer number. In this condition a broad stable regime is experienced. It's clear that dimensions and distances in a feedback structure are fundamental to determine the stability of the whole system.

3.1 Lang Kobayashi Equations

The rate equations of a laser have to be modified if we are in presence of external optical feedback, taking into account the back reflection of the light beam, with new amplitude, phase and delay components.
The new set of differential equations takes the name of Lang Kobayashi equations[15]:

$$\begin{aligned}
\frac{\delta A(t)}{\delta t} &= \frac{1}{2}G_n[n(t)-n_{th}]A(t) + \frac{k}{\tau_{in}}A(t-\tau)\cos(\theta(t)) \\
\frac{\delta \phi(t)}{\delta t} &= \frac{1}{2}\alpha G_n[n(t)-n_{th}] - \frac{k}{\tau_{in}}\frac{A(t-\tau)}{A(t)}\sin(\theta(t)) \\
\frac{\delta n(t)}{\delta t} &= \frac{J}{ed} - \frac{n(t)}{\tau_s} - G_n[n(t)-n_0]A^2(t)
\end{aligned} \tag{3.1}$$

where k is the feedback coefficient and can be written as $k = (1-r_0^2)\frac{r}{r_0}$ with r the reflectivity of the feedback facet and r_0 the reflectivity of the laser facet. τ_{in} is the roundtrip time of the laser cavity, τ is the feedback roundtrip time and θ can be written as $\theta(t) = \omega_0\tau + \phi(t) - \phi(t-\tau)$ taking into account the feedback phase.

With $k = 0$ is easily understandable that no feedback takes place, and we obtain exactly the standard rate equations seen in Equation 2.2.
We can rewrite the Lang Kobayashi equations, expressing the electric field, as

$$\begin{aligned}
\frac{\delta E}{\delta t} &= (1+i\alpha)NE + \eta e^{-i\omega_0\tau}E(t-\tau) \\
T\frac{\delta N}{\delta t} &= P - N - (1+2N)||E^2||
\end{aligned} \tag{3.2}$$

with α the linewidth enhancement factor, η the feedback strength, τ the external delay, ω_0 the angular frequency, T the carrier life time and P the pump current.
We can extract the analytical solution for the Lang Kobayashi equations, obtaining

$$\omega_F(\tau)\tau = \omega_0\tau - Csin[\omega_F(\tau)\tau + atan\alpha] \tag{3.3}$$

where ω_0 is the angular frequency of the laser without external feedback, ω_F is the angular frequency with feedback and C the feedback factor.[16]

3.2 Figures of Interest

3.2.1 Optical Linewidth

The optical linewidth is the width of the power spectral density of the electric field emitted by the laser, measured at the full width half maximum and it expresses the spectral coherence of the laser emission. In a mode-locked laser, noise can affect the amplitude, the optical phase, the central frequency and the frequency spacing between different lines of the comb. The broadening of the comb lines is related to the optical phase noise, given by spontaneous emission, which introduces a Lorentzian shape in all the lines and to the timing jitter fluctuations of the pulses generation.[17]

Our aim is to reduce the optical linewidth of our comb through optical feedback, feeding back to the initial comb a single line with different amplitude and phase, and making them constructively interacting leading to the stabilization of the emission frequency and reduction of the width of the optical spectrum.

3.2.2 RF Linewidth

The RF linewidth is the width of the beating tone of our comb, that can be measured with an electrical spectrum analyzer, it defines how regular the spacing in frequency of the lines is. It is directly related to timing jitter, whose control and reduction is essential to improve the laser performances. Timing jitter is usually defined as the integrated phase noise power spectral density and is expressed by two parameters:

the integrated rms timing jitter:

$$\sigma_T^i(f_u, f_d) = \frac{T_R}{2\pi}\sqrt{\int_{f_d}^{f_u} S_{\Phi RF}(f)df} \tag{3.4}$$

and the pulse-to-pulse rms timing jitter:

$$\sigma_T^{pp}(N) = \frac{T_R}{\pi}\sqrt{\int_0^{+\infty} \sin^2(\pi f N T_R) S_{\Phi RF}(f)df} \tag{3.5}$$

where f_u and f_d are the upper and lower frequency of integration, T_R the period of the pulse train, N the number of periods between the two compared pulses and $S_{\Phi RF}$ the power spectral density of the RF phase noise.
The locking condition guarantees a small time fluctuation of the pulse train, so we can use a first order approximation of the power spectral density of the photocurrent to estimate the RF phase noise. RF frequency noise is induced by broadband spontaneous emission, that can be considered white, leading to the photocurrent first harmonic with a lorentzian shape. We can in this way define

$$S_{\Phi RF}(f) = \frac{\Delta\nu_{RF}}{\pi f^2} \tag{3.6}$$

leading to a pulse-to-pulse rms timing jitter of

$$\sigma_T^{pp}(N) = T_R\sqrt{\frac{\Delta\nu_{RF} N T_R}{2\pi}} \tag{3.7}$$

and the integrated rms timing jittering

$$\sigma_T^i(f_u, f_d) = \frac{T_R\sqrt{\Delta\nu_{RF}}}{2\pi^{\frac{3}{2}}}\sqrt{\frac{1}{f_d} - \frac{1}{f_u}} \tag{3.8}$$

With some approximations[18] we can rewrite RF linewidth as

$$\Delta\nu_{RF} = 2\frac{\tau^2}{T_R^2}(0.53 + 0.01\frac{D^2\Delta f_g^4}{g^2})\Delta\nu_{ST} + \frac{\gamma^2}{T_R^2}RIN \tag{3.9}$$

with τ the full-width half maximum of the hyperbolic secant pulse, result of the Haus master equation for a mode-locked laser, g the saturated intensity gain per round trip, D the group delay dispersion, Δf_g the gain bandwidth, $\Delta\nu_{ST}$ the optical linewidth and γ the coupling factor from energy to timing fluctuations.
As we can see the RF linewidth is the sum of three contribution, amplified spontaneous emission, the conversion of optical frequency fluctuation in RF frequency noise by dispersion and the conversion of RIN in RF frequency noise due to fast gain changes.

3.2.3 RF and Optical Linewidth relation

As we have seen, both optical and RF linewidth are fundamental parameters to define the stability of our laser. It's interesting to study the relation between these two figures. In a passive quantum dash mode-locked laser, the optical linewidth of different lines is varying with a parabolic shape, as wee can see in Figure 3.2.
The parabolic increase of optical linewidth can be directly related to the RF linewidth with the relation

$$\Delta\omega_n = \Delta\omega_0 + \Delta\omega_{RF}(n - n_0)^2 \tag{3.10}$$

where $\Delta\omega_0$ is the optical linewidth of the fundamental line, $\Delta\omega_m$ is the optical linewidth of the n^{th} line and $\Delta\omega_{RF}$ the RF linewidth. We can in this way

relate the aperture of this parabolic shape directly to the RF linewidth of the whole comb, relating this two important parameters.[19]

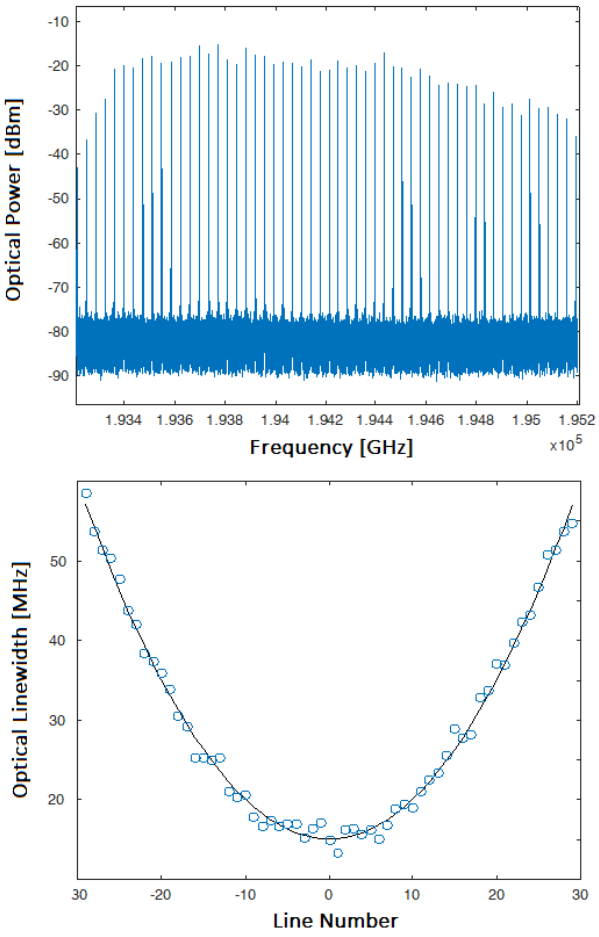

Figure 3.2: Parabolic dependance of optical linewidth of different lines of a passive quantum dash mode-locked laser.

Chapter 4

Setup and PIC Description

4.1 Structure

Our integrated circuit implements an optical feedback loop, whose main goal is to improve the properties of our mode-locked laser. In particular the feedback structure is composed by two separate branches, accessible through ring resonators, each provided with phase tuners and a sagnac-loop to reflect back the light and always through the ring again into the laser.

As we can see from the block diagram scheme in Figure 4.2, the input light goes directly into the rings, that are tuned in such a way to filter selectively two lines of the comb. These two single lines are redirected in the two branches of the feedback structure, where they experience a phase tuning and then are totally reflected back by the sagnac-loop again into the ring and back to the laser.
The goal is to create constructive interference between the comb laser and the two fed-back lines, investigating if the optical feedback can be beneficial in terms of stabilization of the source laser. Since the system is really sensitive to thermal and mechanical fluctuations, we provided both the laser and the chip with a temperature controller, to guarantee maximum stability.

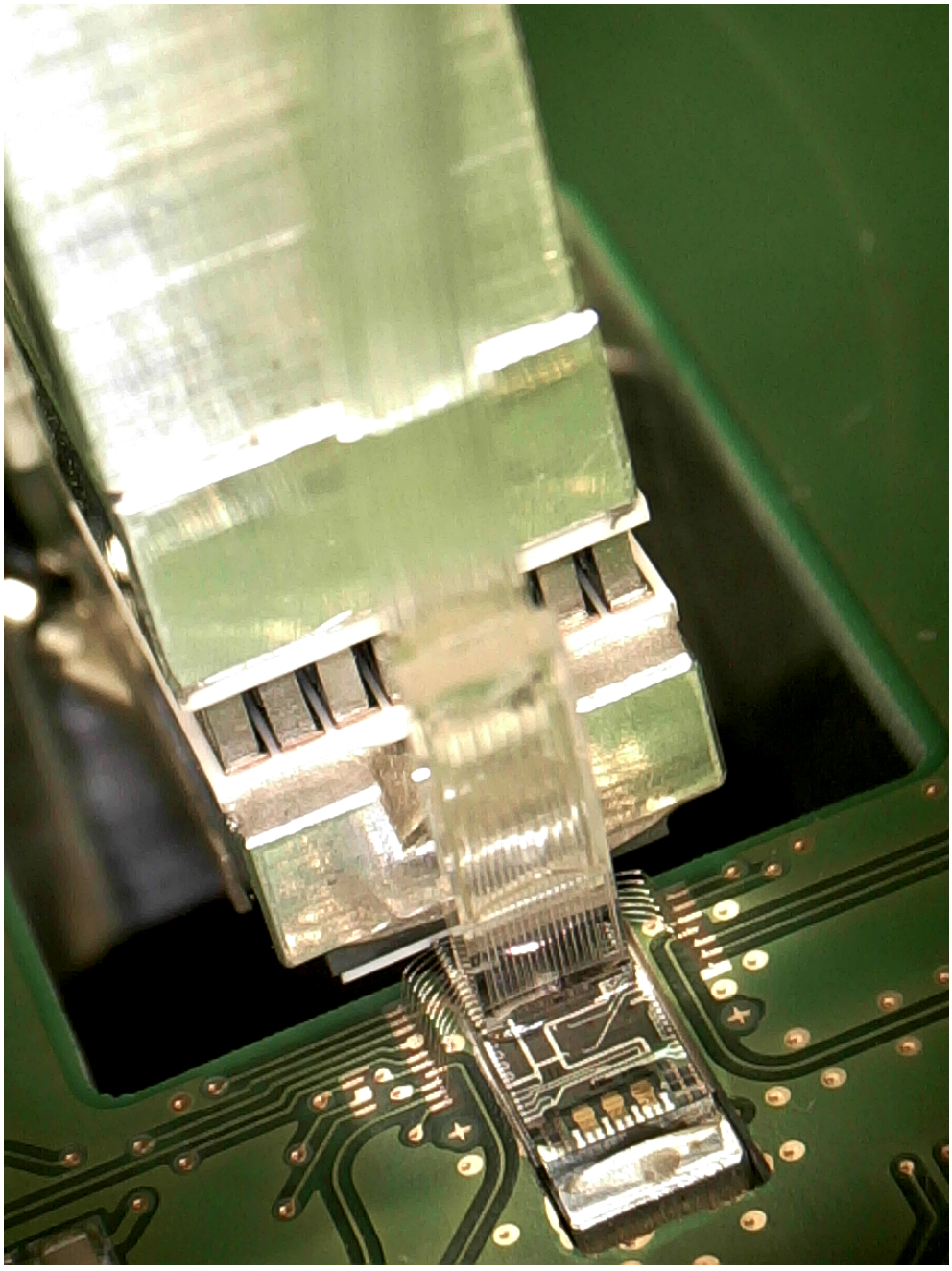

Figure 4.1: Set Up. Main elements are the laser mounted under the piezoelectric actuator, with its temperature controller, the photonic chip wirebonded to the printed circuit board and the optical fiber array attached to the PIC.

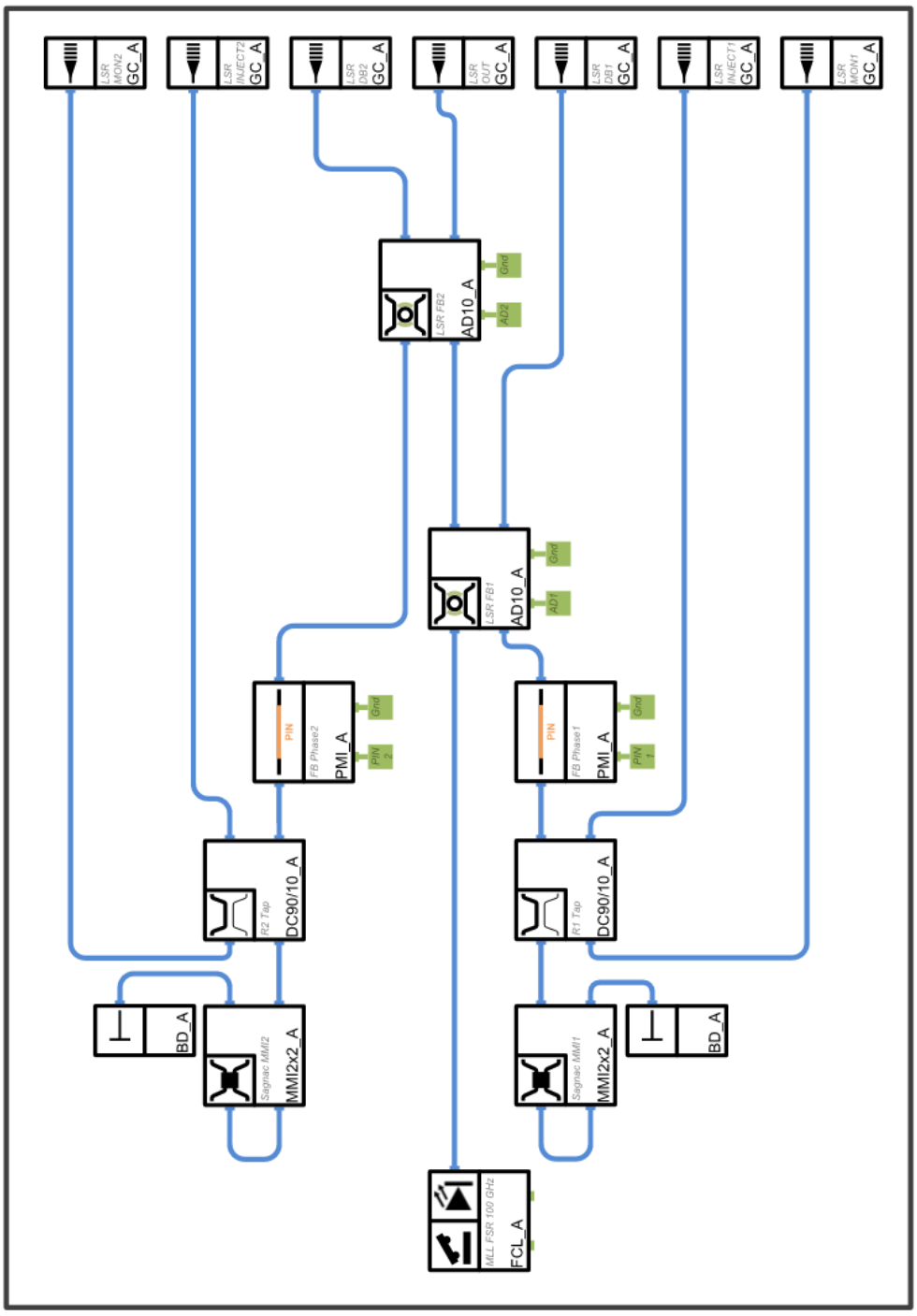

Figure 4.2: Photonic Integrated Circuit layout.

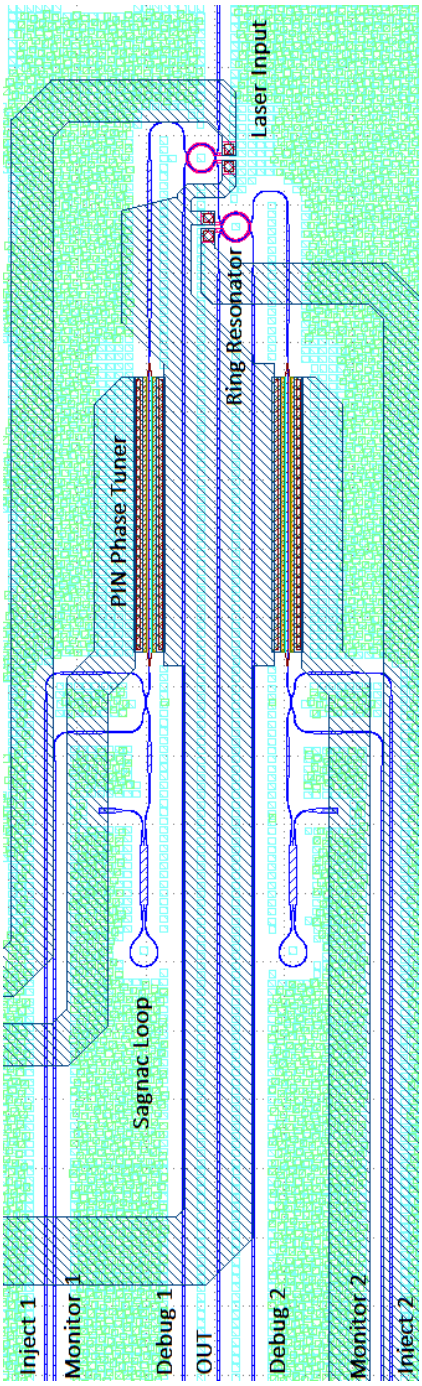
Inject 1
Monitor 1
Debug 1
Sagnac Loop
PIN Phase Tuner
OUT
Ring Resonator
Laser Input
Debug 2
Monitor 2
Inject 2

4.2 Laser

The main element of our measurement set up is the laser source. It is a semiconductor quantum dash passive mode-locked laser. The comb shaped spectrum range is between 1535 nm and 1555 nm, in the telecommunication wavelength range, with a band of 2.5 THz. The Free Spectral Range (FSR) of the laser, i.e. the spacing between two neighbor lines of the comb, is 36.7 GHz, so we have in total 55 lines.
To characterize the laser, first of all we ran a sweep of the laser current to see how the spectrum change in function of its bias current. The measurement was performed with a temperature of 30°, kept constant with a Thermoelectric Controller, the result can be seen in Figure 4.3.

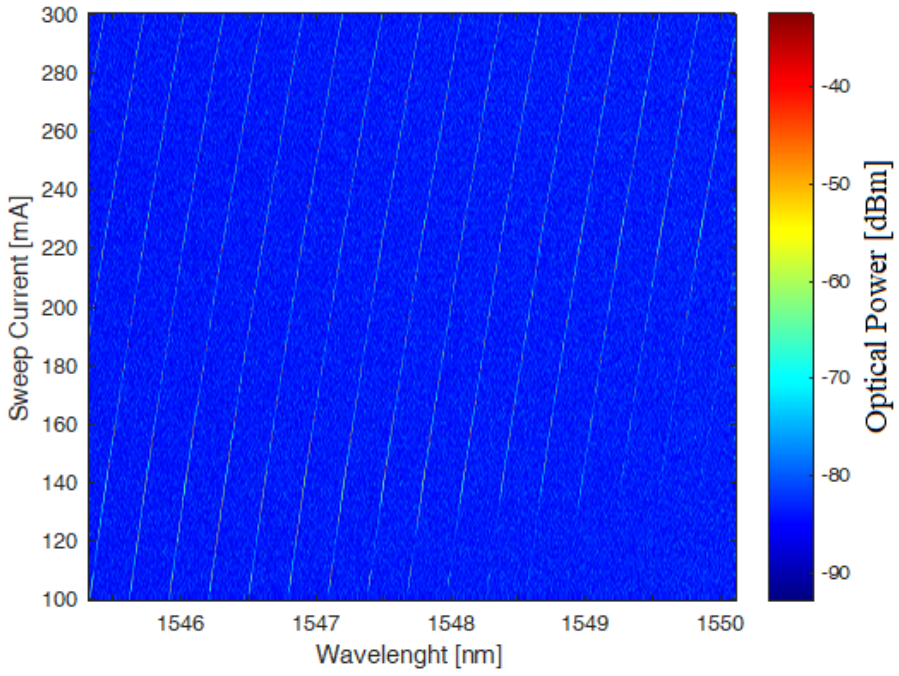

Figure 4.3: Laser Spectrum at different bias currents.

Now we can analyze for each current spectrum the optical linewidth of the lines of the comb to understand which operating point gives a good locking condition. To do this we simply fit every line of the comb with a lorentzian and compute its linewidth.

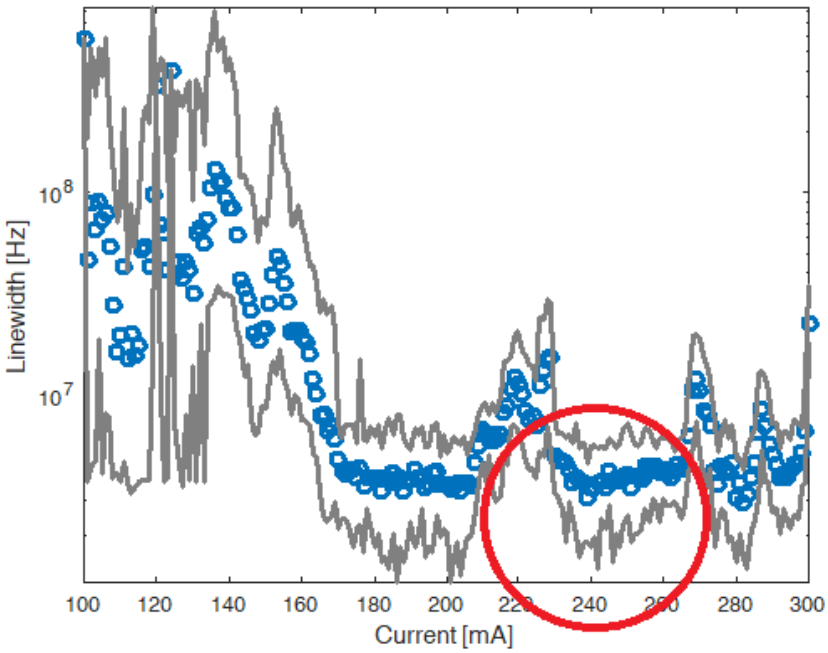

Figure 4.4: Optical Linewidth of the laser at different bias currents. The upper gray line shows the maximum optical linewidth of the comb, while the lower gray line the minimum. In blue dots we can see the average optical linewidth of all the lines.

As we can see in Figure 4.4, we can choose the working point of the laser where the optical linewidth is low and it has a wide range, meaning that the locking condition is good and stable in case of current fluctuations. So for our measurements we selected a bias current of 240 mA for the laser.
The optical spectrum, measured with an optical spectrum analyzer, at this working point is shown in Figure 4.5 and it presents an average optical linewidth of 3.5 MHz.

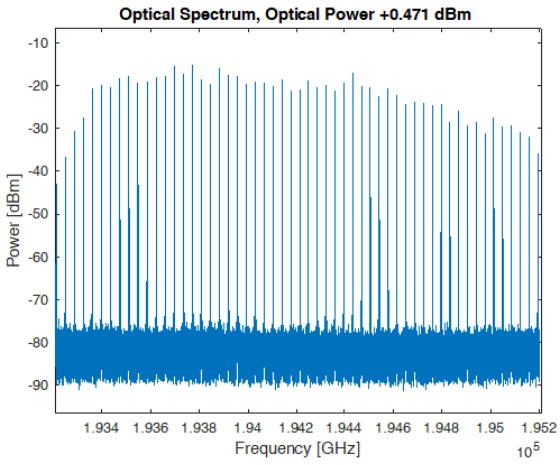

Figure 4.5: Optical Spectrum of the free-running laser at 240mA.

We also measured the RF Spectrum of the free-running laser with an electrical spectrum analyzer, measuring the beating tone of the comb at different laser's currents and we obtained an RF Spectrum with an RF Linewidth of 9 KHz at the operating current of 240mA.

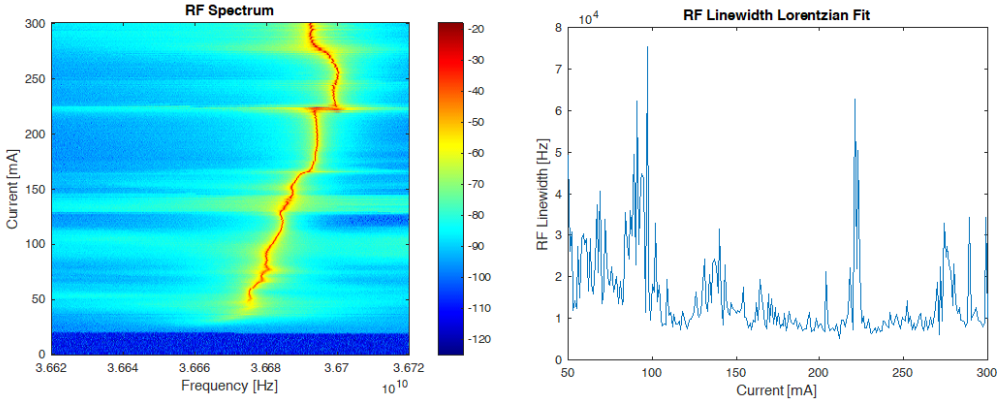

Figure 4.6: RF Spectrum of the free-running laser at different currents and RF Linewidth for each current, computed through Lorentzian Fit.

4.3 Coupling

We face a direct coupling between the laser and the chip, which is challenging since we want to get as close as possible to the chip coupler, but avoiding a collision between laser and chip, even if this last one is provided with bumpers. To compute the right coupling distance we used a Gaussian beam approximation for our laser and calculated the Rayleigh length of our beam taking the -3dB width using a powermeter at the output. In this way we are able to estimate the real distance between laser and chip facet and actuate the piezoelectric controller in the correct way. But at really short distance, this approximation doesn't hold anymore. Since losses are an important contribution in direct coupling, we implemented an inverse tapered coupler on the chip to have a better coupling efficiency, lower losses and wider bandwidth. Inverse tapers use a tapered waveguide to form the optical mode profile, whose dimension smoothly varies in an adiabatic condition to avoid the excitation higher-order modes and consequent losses.[20]

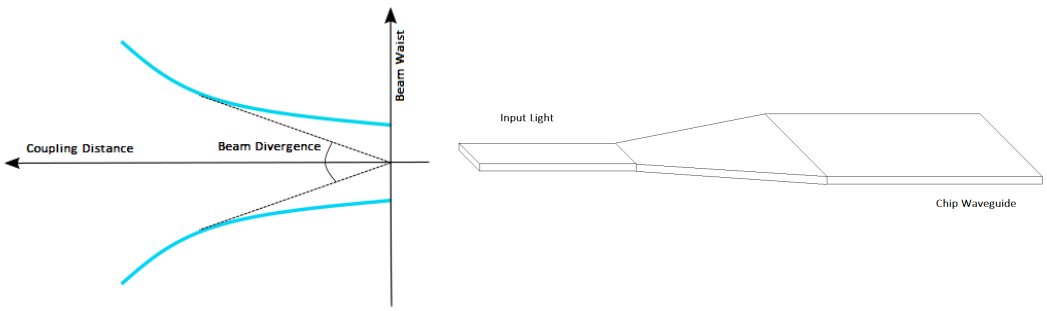

Figure 4.7: Gaussian beam approximation on the left, Inverse tapered edge coupler on the right.

4.4 Photonic Devices

4.4.1 Ring Resonators

A ring resonator is a photonic device made of an optical waveguide with a circular shape, placed in proximity to one or more straight waveguides to allow coupling, i.e. to allow the light coming from the straight waveguide to enter the ring itself. Once inside the loop, the light will circulate accumulating a phase according to the ring length and when it reaches the initial point, if it is in phase with itself it constructively interferes giving place to resonance. This happens when the optical path of the ring is an entire multiple of the wavelength. Thanks to the high refractive index contrast between silicon and silicon oxide, single mode waveguides can be bent with a radius lower than $5\mu m$ so they have quite a small size, a very relevant factor in silicon integrated circuits.

As said, the working principle of a ring resonator is based on coupling mechanism which allows the light to access the fiber loop from a nearby waveguide. The propagating wave is, in fact, not entirely confined inside the waveguide, but can be partially outside as evanescent wave. If two waveguides are close enough, this evanescent wave can reach the second guide before its extinction, be coupled and so transmitted as a normal wave into this second guide. Thanks to this mechanism, the light coming from a straight waveguide can enter the ring and reach the resonance condition. The output of a ring resonator will be a notch filtered version of the input spectrum, where the frequencies that respect the phase condition and so resonate, are removed.[21]

This is the working principle of an all-pass ring resonator. We usually use an add-drop ring resonators, where two different optical waveguides are coupled to the loop, with two inputs and two outputs and a double coupling mechanism, as we can see in the picture below. At the through port the filtered version of the input spectrum will be the output, as in the all pass ring, while at the drop port we can find the frequencies that resonate in the ring, so basically the reciprocal function. The add-drop structure gives also

the possibility to add, through the add port, a new spectral component at the through port, substituting the one filtered out by the ring.

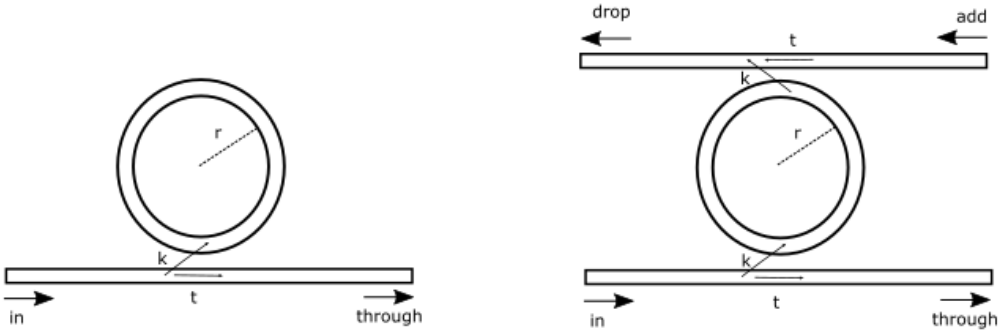

Figure 4.8: All-pass ring resonator on the left, Add-drop ring resonator on the right.

The transfer function for the all-pass ring is the following

$$T = \frac{I_{pass}}{I_{input}} = \frac{a^2 - 2ta\cos\Phi + t^2}{1 - 2at\cos\Phi + (ta)^2} \tag{4.1}$$

which implement a notch filter function, while for the add-drop ring

$$\begin{aligned} T_p &= \frac{I_{pass}}{I_{input}} = \frac{t^2a^2 - 2t^2a\cos\Phi + t^2}{1 - 2t^2a\cos\Phi + (t^2a)^2} \\ T &= \frac{I_{drop}}{I_{input}} = \frac{(1-t^2)^2a}{1 - 2t^2a\cos\Phi + (t^2a)^2} \end{aligned} \tag{4.2}$$

where $\Phi = \beta L$ is the ring phase shift, with L the round trip length and β the propagation constant. a is the amplitude of transmission taking into account losses $a = \sqrt{exp(-\alpha L)}$ and $t^2 + k^2 = 1$ where t and k are the power splitting ratio of the coupler.

As already mentioned, one of the application for a ring resonator consists

in spectral filtering according to the resonance frequency. Only a limited range of wavelengths can pass through the ring and be transmitted to the drop port. In photonic circuits, they are useful also to implement an optical delay line, in fact, near the resonance there will be strong dispersion, causing a large group delay. The most interesting application, is however reached with an active usage of ring resonators. We can in fact modulate the effective index in the ring modulating the temperature, through a thermal heater structure placed on top of the ring.This is quite a slow process, if we want a faster response we can also change the carrier density through carriers injection in a PIN junction. This alternative is faster since the time constant is given by the junction capacitance and will result much lower, but with more carriers we will have more losses due to scattering phenomena, so we use thermally tunable rings in our circuit, as we can see in Figure 4.9.[22]

These are the specifications of the ring resonators used in our photonic integrated circuit:

Radius	$10\mu m$
Bandwidth (-3dB)	6 GHz
FSR	1.1 THz
Reflectivity	0.076

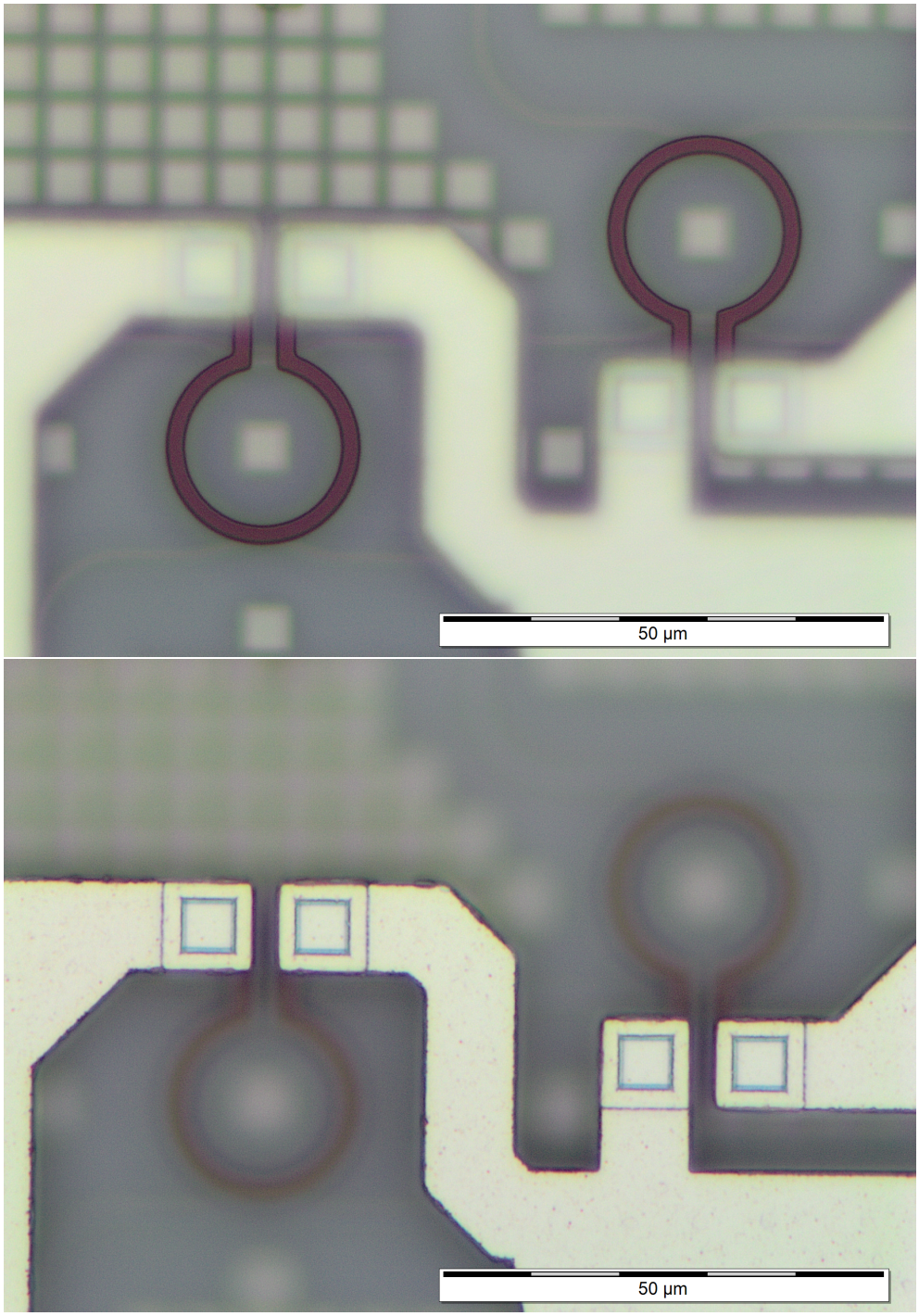

Figure 4.9: Ring Resonators. In the upper picture we can see the ring thermal heater structure, while in the bottom picture the electrical contacts on a different layer are focused.

4.4.2 Phase Shifter

In lots of applications is fundamental to be able to adjust the phase of our optical signal, for example for signal modulation or to reach phase matching condition. To achieve this goal a simple photonic device is available, known as phase shifter. We can change the propagation constant modulating the refractive index of the waveguide, leading to a change in the phase of the optical signal that passes through it with the well known relation

$$\Delta\phi = \Delta\beta L = \frac{2\pi}{\lambda}\Delta n_{eff} L$$

$$with \tag{4.3}$$

$$\Delta n_{eff} = \frac{1}{Z_0}\frac{\int n\Delta n E E^* dA}{\int |ExH^*| Z dA}$$

where the refractive index n is defined as the ratio between the velocity of light c and the phase velocity of our optical beam. It is evident that the refractive index contains information about the phase of our signal, and modulating it properly, we can obtain a phase modulation as direct effect.
There are mainly two ways of implementing a phase shifter, using a PIN junction or a thermal shifter.

In a **PIN junction**, changing the bias voltage, we can change the carriers density, leading to a modification of the refractive index of the junction itself due to band filling effect and free-carrier absorption.[23]
We can express the variation in carrier density as

$$\Delta N(E, n) = \Delta N_{BF}(E, n) + \Delta N_{FCA}(E, n) \tag{4.4}$$

The band filling effect takes place when the concentration of carriers is increased. These exeeiding carriers occupy the low energy states of the bands

and consequently we will experience a modification of the actual energy band gap, since transitions between these occupied states will be forbidden. In doped silicon, also free-carrier absorption has a consistent effect. When the carrier concentration is high, is more likely that a photon is absorbed by the material, and an already excited carrier is excited to another unoccupied energy level. This phenomenon leads to a modification of the carrier distribution in the energy levels and a consequent reshaping of the energy gap. These two effects, changing the energy gap of the material, will influence and change also the refractive index.[24]
The phase shift generated by this kind of junction is really fast, since it involves carrier density modulation, actuated through an electrical signal, but presents also a disadvantage. It causes, in fact, quite a lot of reflections of the optical signal because of the large amount of free-carriers that induces scattering phenomena.

The working principle of a **Thermal phase tuner** is again based on refractive index changing, but this time induced by a change in temperature, according to this relation

$$\frac{dn}{dT} = (\frac{\delta n}{\delta T})_\rho - (\frac{\rho \delta n}{\delta \rho})_T(\gamma) \tag{4.5}$$

that shows a refractive index dependence on temperature through a direct temperature-induced change in the density ρ, assuming γ the coefficient of volume expansion.
This method guarantees a phase shift of our optical signal with almost no reflection, since no carrier density modulation is involved, however it presents also a drawback. The process is, in fact, much slower with respect to a PIN junction phase modulator, because temperature change requires more time to be actuated.[25]
In our photonic circuit we use PIN phase shifters to have a fast response, long $200\mu m$ which guarantees a phase shift of $\frac{\pi}{4}$ applying a current of 5mA.

4.4.3 Sagnac Loop

In a close loop system one of the most important element is the reflector. We need, in fact, a device that is able to totally reflect back the light into the main branch. For this purpose, we use a Sagnac loop reflector which is basically a 2x2 directional coupler whose outputs are connected with a piece of fiber in a loop configuration, as shown below.

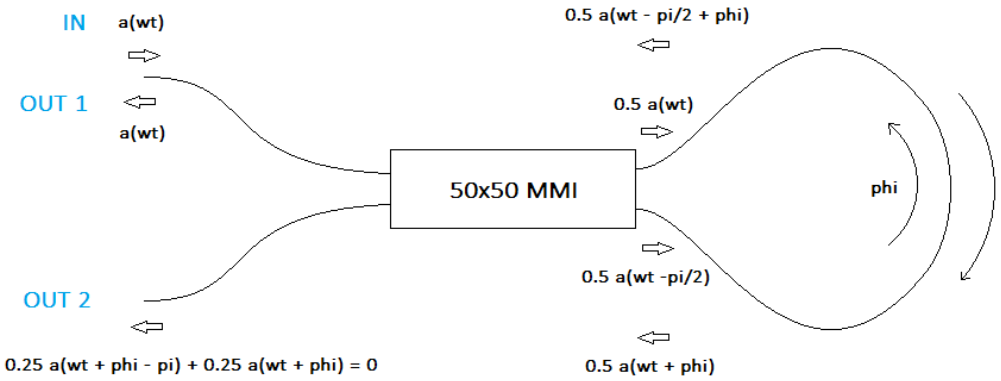

Figure 4.10: Sagnac Loop total reflector structure.

If light is fed into one of the input ports, the power is split so that two counterpropagating waves are generated into the loop. When these two waves come again at the coupler, they interfere with each other, determining the optical power sent out to the two ports. We want to implement a total reflector so we choose a directional coupler with a 50:50 power splitting ratio so after entering it from one input (suppose the upper one), half of our optical power will travel clockwise in the fiber loop, and the other half counterclockwise with a $\pi/2$ phase shift due to coupling. When the two counterpropagating waves meet again at the directional coupler, they will have gained the same phase ϕ proportional to the loop length. The output not connected to our circuit (the lower one) will be the sum of a clockwise field with the arbitrary phase ϕ and a counterclockwise field with phase $\phi - \pi/2 - \pi/2$, where the second $\pi/2$ is given again by a second coupling, giving place to a completely destructive interference. It is evident that the lower output will present zero transmitted energy and, due to energy conservation, neglecting the losses, the upper output will transmit the whole input signal, revealing a total reflector transfer function.[26]

4.4.4 Grating Couplers

Finally, also grating couplers are fundamental devices because they allow to couple light from the planar SOI waveguides in our PIC to external optical fibers. As shown in the circuit block diagram, we have an array of grating couplers which allows the attachment of an optical fiber array to read each output of our circuit. We have implemented grating couplers with an adiabatic taper to guarantee mode field adapting through a slow variation of the parameters of the waveguide and optimizing the coupling efficiency with the grating.[27] In the grating itself, thanks to the refractive index modulation, diffraction takes place and our light beam is steered perpendicularly, or with a steering angle, to the waveguide. It's now possible to couple an external optical fiber on top of the grating, with the same steering angle, and connect it to our measurement tools.

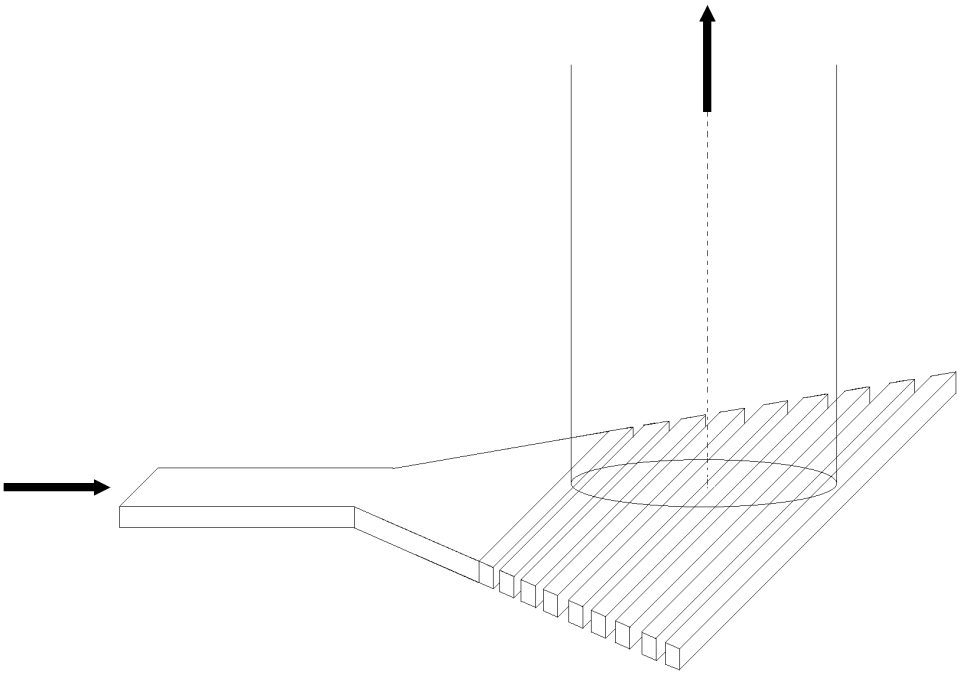

Figure 4.11: Grating coupler for coupling between integrated waveguide and optical fiber.

Chapter 5

Experimental Results

5.1 Devices Characterizations

In order to be able to properly control the optical circuit, we need to characterize each photonic device in our PIC. First we use a broadband lensed fiber and a circulator which allow us to know the optical response of each device to the electrical supply, measuring the back reflections. We inject light in the circuit from the input port and observe the changings of the devices spectral response to different tuning currents, like the shift in frequency of the rings resonance at different injected currents in the ring thermal modulator or the phase shift provided by the phase tuners at different modulating currents.

5.1.1 Ring Resonators Characterization

In our filtered tunable optical feedback ring resonators are fundamental, since they provide the spatial filtering needed to isolate one single line of the comb and let it enter the feedback branch. It's then really important to know exactly how the rings behave and how we can tune them. As already discussed

these rings are provided with a thermal modulator, so injecting a current, through thermal effect, we can shift the ring resonance in frequency. To characterize the ring we need to measure its spectral behavior at different injection currents. As first measurement, we couple a lensed fiber with circulator at the input of the PIC to inject light in the photonic chip and measure the back-reflections, which will show the presence of the ring.

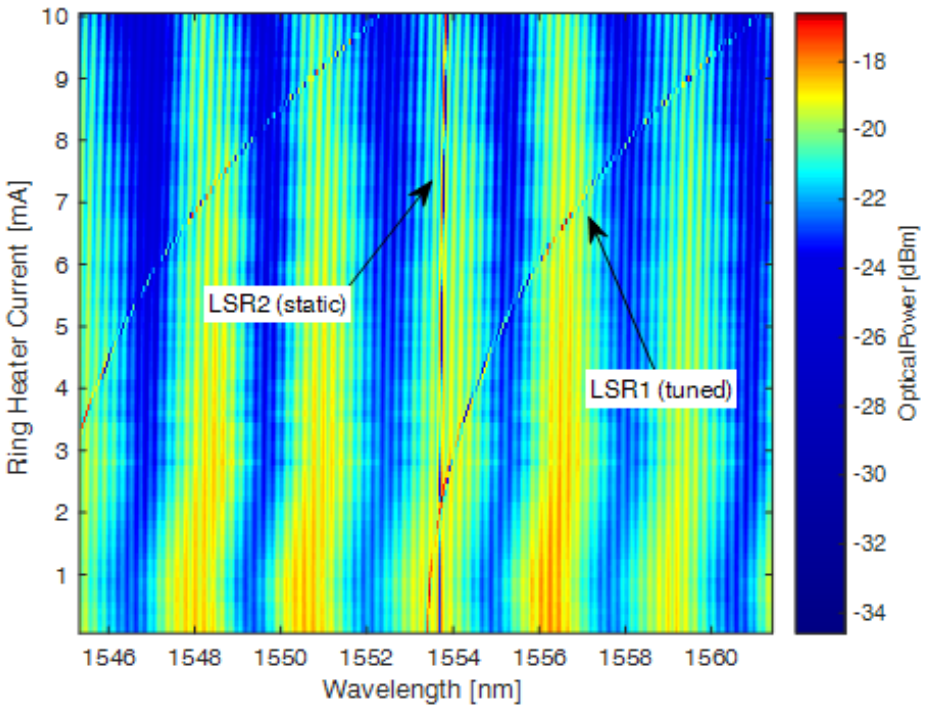

Figure 5.1: Chip back-reflection with ring thermal heater current sweep.

In Figure 5.1 we can see the Optical Spectrum of the back-reflections at different tuning currents for the first ring resonator, while the second is kept static at 0mA. We can clearly see how the thermal effect shifts the ring resonance through higher wavelengths. This will make us able to tune the ring really precisely in order to filter different lines of the combat different frequencies. In the second Figure, single currents optical spectra are shown.

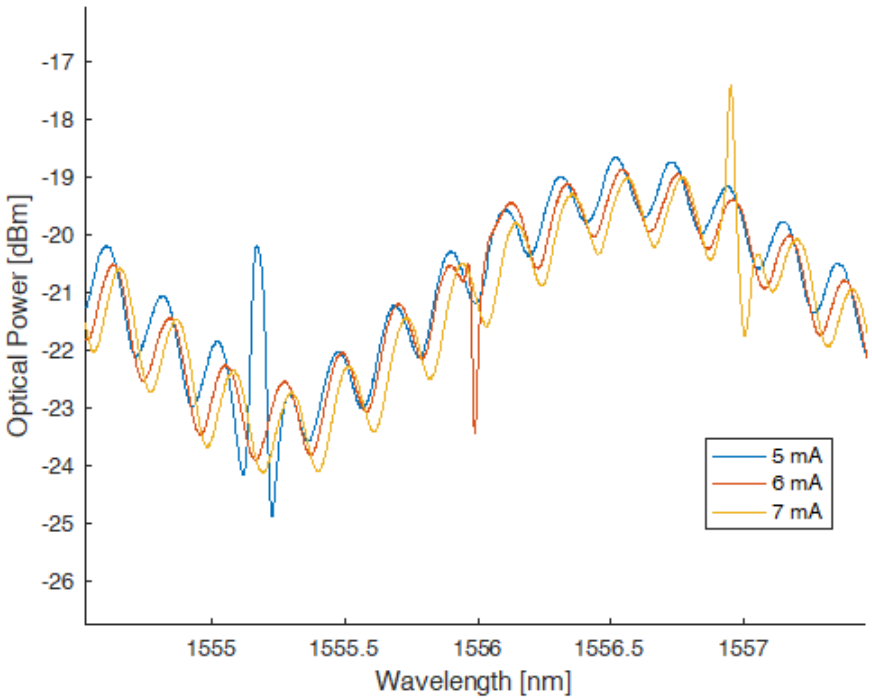

We can also analyze the ring transfer function injecting light from the Debug port of the circuit and reading the optical spectrum directly at the output of the chip, as shown in Figure 5.2.
Here the characteristic of the ring resonator at the drop port is shown and once again we can see how, at different heating current the resonance is shift through higher wavelengths, making possible the filtering of a specific line of the comb line as we will see in next measurements.

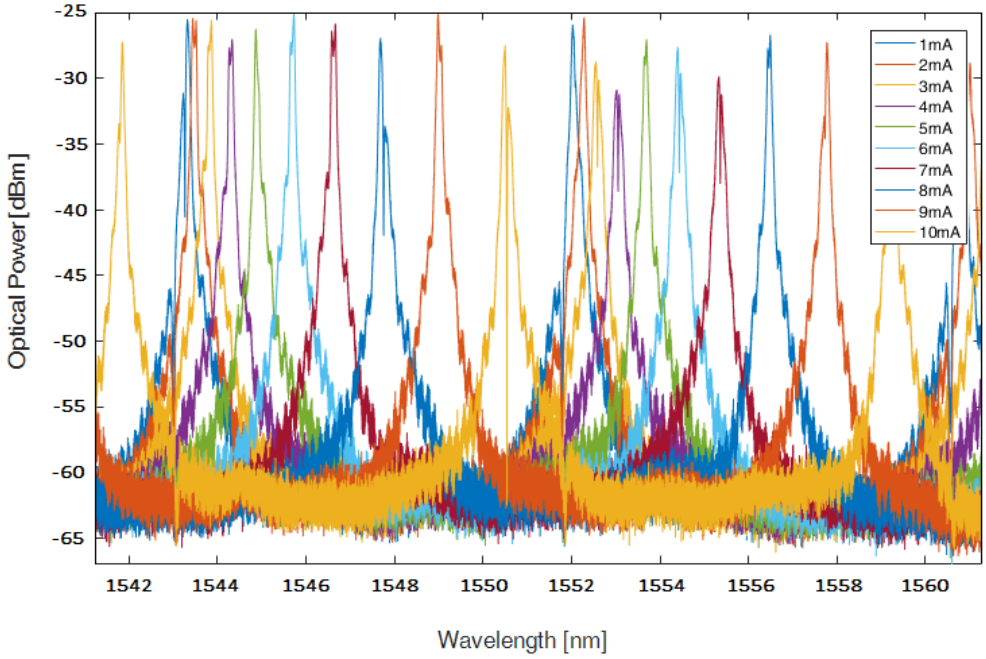

Figure 5.2: Ring resonance at different thermal heater currents.

5.1.2 Phase Shifters Characterization

The next devices we need to characterize are the PIN phase shifters, once again applying a certain injection current in the PIN junction, we will experience a phase shift in the light going through it, and we want to know the exact current-phase shift relation in order to actuate properly the device. We use again the lensed fiber with circulator to measure the back-reflections from the chip and, applying different currents to the phase tuner, we measure the periodicity of the device.

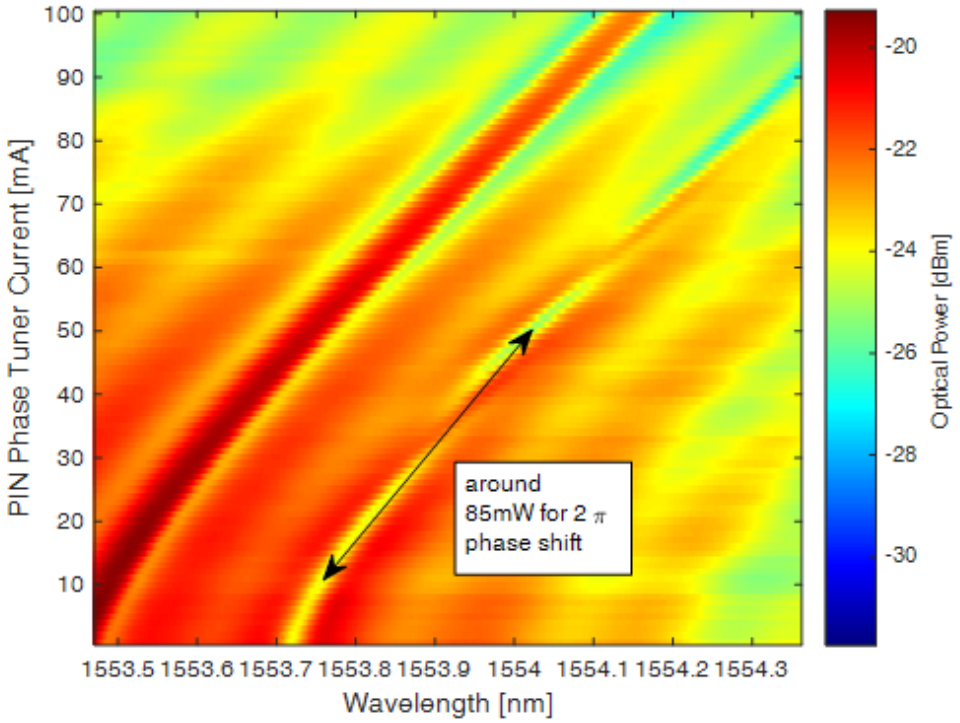

Figure 5.3: Back-reflections spectrum tuning the PIN phase tuner current.

The light measured is given by the interference between the injected and the back-reflected light and, applying a different phase shift, the interference switches between constructive, where the power sums up, and destructive, where the power drops. In Figure 5.3 it's clear how the power measured oscillates in a periodic fashion, so we can extrapolate the periodicity of the phase tuner, that applies a 2π phase shift every 40mA applied. In the graph, the shift through higher wavelengths of the line taken into account can be easily explained by general thermal heating of the chip.

5.2 Analysis with Mode-Locked Laser

5.2.1 Laser Spectrum Alignement

Now that we know the response of every component singularly, we can couple the mode-locked laser to the chip and look at the overall effect. To do this, we need first to align the comb-like spectrum with the ring transfer function in a proper way, to avoid that the rings, which have an FSR of 1.1 THz, take simultaneously more than one line of the comb each. We want to avoid it because it would increase the level of complexity of our system. For now we want to analyze the effect of optical feedback with one single line in each branch.

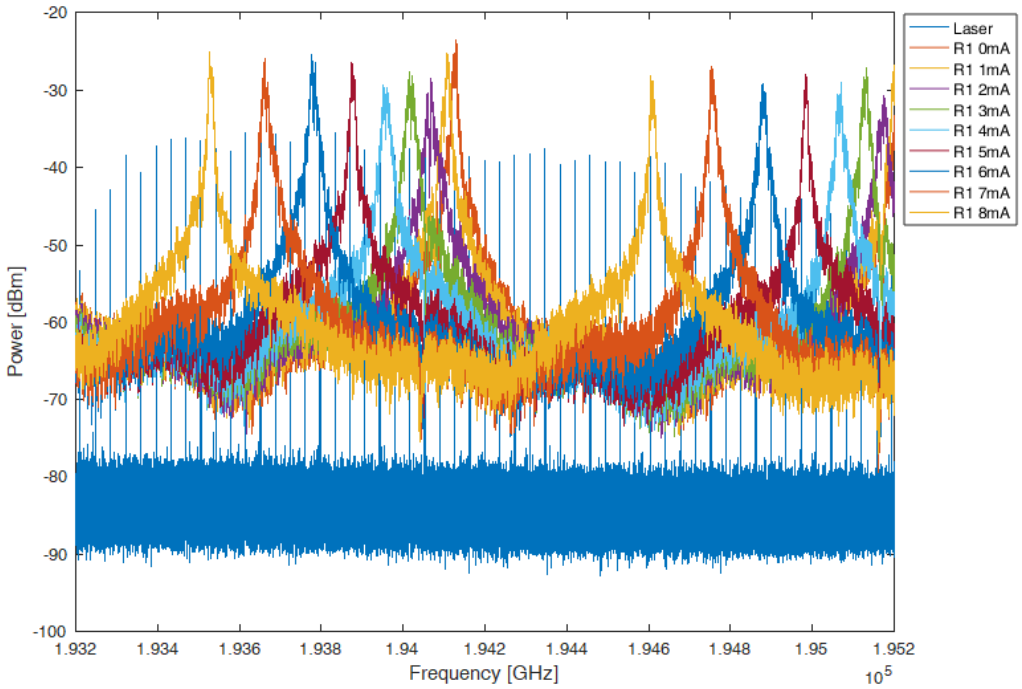

Figure 5.4: Comb spectrum alignement with the ring transfer function.

As we can see in Figure 5.4, the laser has been aligned in a way that all the high power lines are in the first frequency range of the ring. Since the spectrum of the laser is wider with respect to the ring FSR, some lines will also fall in the second resonance range, but properly aligning the laser, we can place in that regions the low power lines, guaranteeing a much weaker effect.

5.2.2 2D Rings Heater Current Scan

The first interesting results were achieved running a double sweep of the two ring resonators heater currents and measuring the RF spectrum and the optical power at the output of the chip. From the optical power graph, we can observe how the line of the comb laser that is filtered by the ring change by changing the current of the ring, looking at those points where the power drops. First we ran a sweep between 0 and 5 mA to observe the general behavior, and we found, as we can see in Figure 5.5, a grid pattern for optical power and RF linewidth given by the entering of different lines of the comb into the feedback branches. We can observe that the locking condition of the laser changes, depending on which line is filtered. The reflection of some of them badly influences the laser, resulting in a broadening of the RF linewidth, while some others have a narrowing effect.

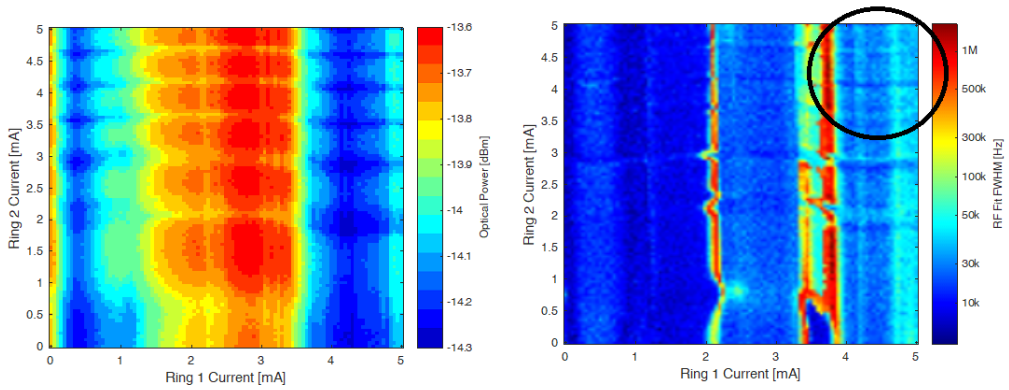

Figure 5.5: 2D Scan of ring resonators heater current.

At this point we decided to focus the measurements in a range of ring heater currents between 4 and 6 mA where, from previous measurements, the effects of feedback where more pronounced. With an higher resolution, we can observe again this grid pattern, given by different resonances, and find really interesting points where the RF linewidth is reduced to the order of 3kHZ, as we can see in Figure 5.6.

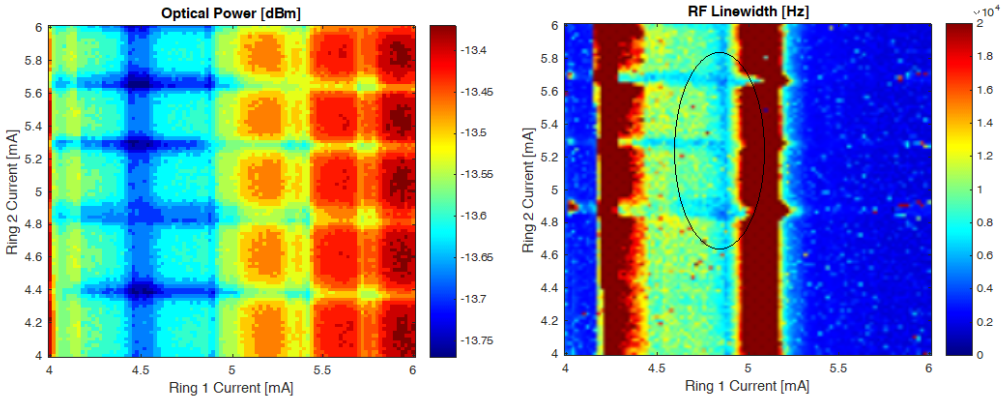

Figure 5.6: 2D Scan of ring resonators heater current.

It is also interesting to notice that these points correspond to Ring 1 filtering always the same line and Ring 2 filtering direct neighbor lines to that one.
If we compare the low linewidth obtained to the one of the free-running Laser, we can observe a reduction of a factor 3, not really significant but enough to state that the filtered optical feedback guarantees a stable operating point of the mode-locked laser, improving slightly its performances.
As we discussed in Chapter 2, we can fit the RF spectrum, not only with a simple lorentzian function as in the previous results, but also with a functions that implement a lorentzian shape for the flanks of the spectrum and a flat plateau on top of it, to model independently phase noise and frequency fluctuations. We want, in fact, to analyze the effect of feedback on phase noise, so this second fit is more useful to have a better understanding of it.

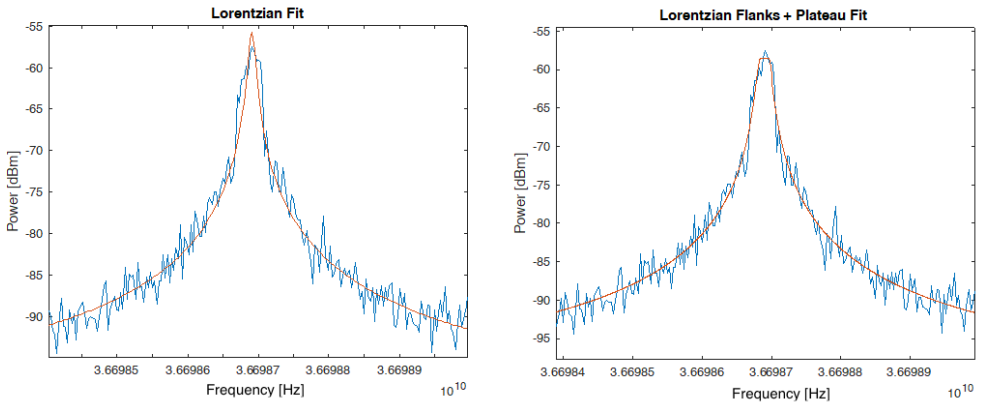

Figure 5.7: Comparison between lorentzian fit and modified lorentzian with a flat plateau to model independently noises effects.

This will lead to a new data set for the RF linewidth, where the beneficial effects of feedback are still visible and related directly to reduction of phase noise in the laser. From this point on, on plots will be presented the RF linewidth computed with this method, to represent the effective phase noise.

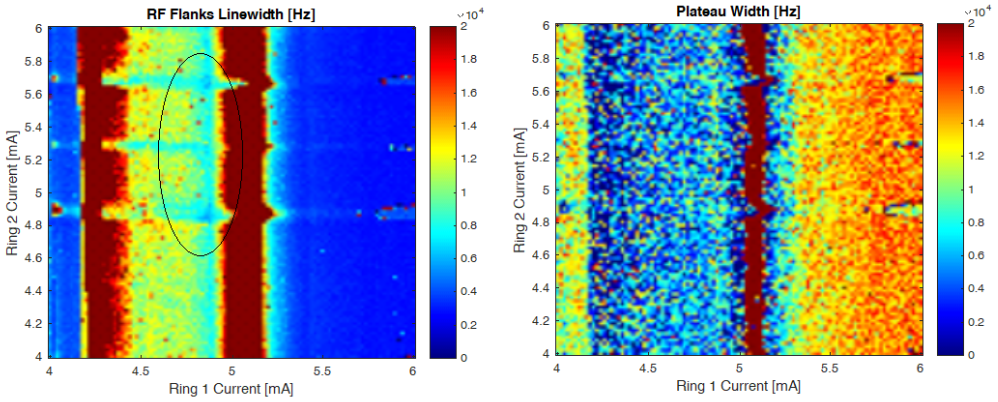

Figure 5.8: RF linewidth and Plateau width with the new fit.

5.2.3 2D Scan changing the Laser bias current

We are now interested to understand if we can exploit the feedback effects starting from an already bad locking condition of the free-running laser and trying to improve it. We switch the bias current of the laser from 240mA, which was the best and most stable operating point of the laser, to 270mA and from the previous laser characterization, we can see that now both optical and RF linewidth are worse, the first around 10MHz the latter around 20kHz.

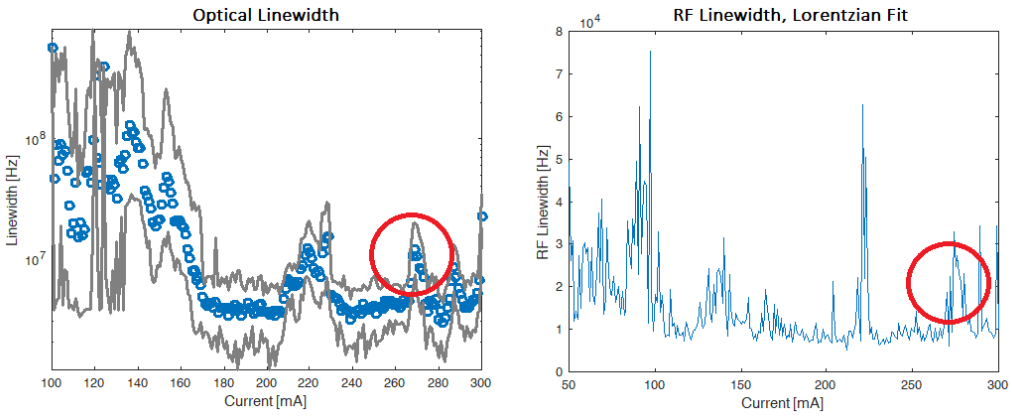

Figure 5.9: New Operating point of the Laser.

We ran again the two dimensional sweep of rings heater current, directly in the 4 to 6 mA range, since we have already seen the beneficial effect when filtering those lines, and we can observe the results in Figure 5.10.

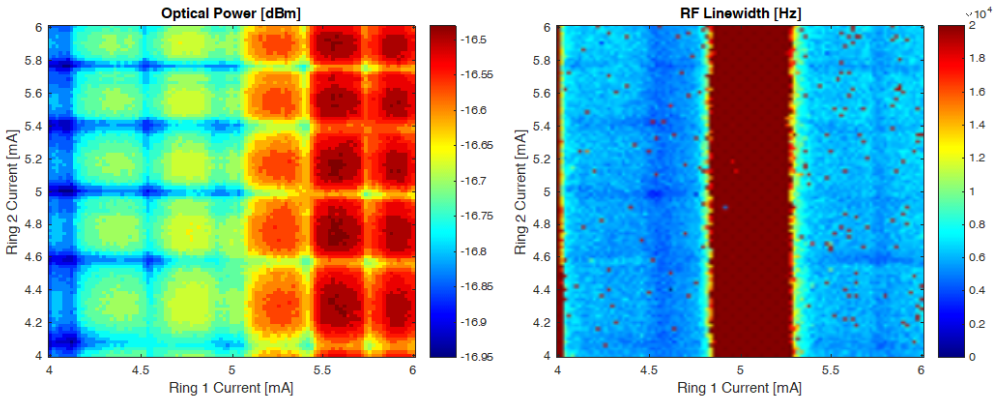

Figure 5.10: 2D Scan of ring resonators heater current in a different Laser operating point.

We can still observe the grid pattern given by different resonances and the beneficial effect in terms of linewidth reduction. It is interesting to notice that this time we experience improvements also when other lines are filtered by the rings, since the starting locking condition is worse then before and there is more room for improvement. In this case the RF linewidth drops below 3kHz and, considering that at this operating point, the laser presents a 20kHz linewidth, we can see that the overall effect is more consistent.

We then measured the optical spectrum of the laser with ring 1 at 4.5 mA and ring 2 at 5 mA, i.e. in the good RF linewidth point, to check if we have an improvement also in the optical linewidth. We discussed in Chapter 3 the relation between the two, and, in fact, we found out that also the optical linewidth is reduced, from an initial value of 10 MHz to a value around 2.5 MHz. Again, the improvement is not significantly high, but it shows the positive effect of external feedback.

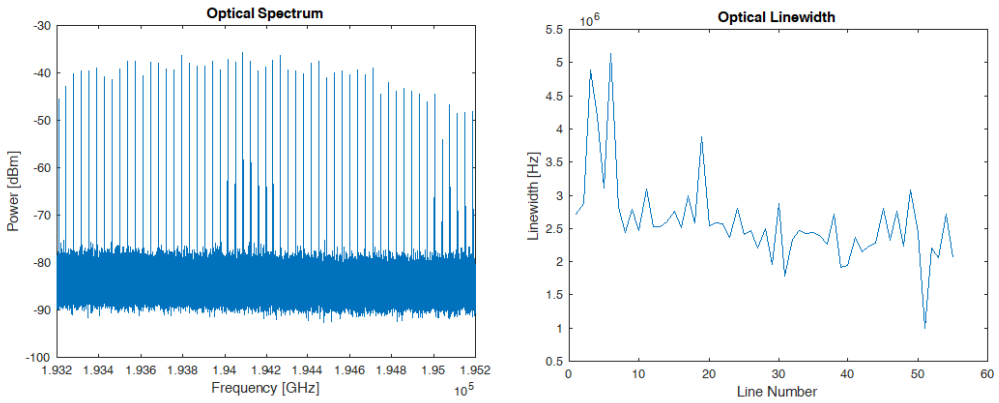

Figure 5.11: Optical spectrum in a good feedback operation point and Optical Linewidth of each line.

5.2.4 Rings and Phases Current Scans

Given these good results, we want now to act on the phase tuners and investigate if, with a proper phase shift, we can reduce even more the laser linewidth. We decided to focus on the points where the effect of optical feedback is more pronounced, as already discussed, and run with the same resolution the 2D scan of ring currents, this time applying also a constant current to the phase tuners for each scan, actuating in this way a phase shift of the lines filtered by the rings. We can take the previous results as reference of 0 phase shift, since we were not acting on the phase tuners, applly different currents to them and compare the results.

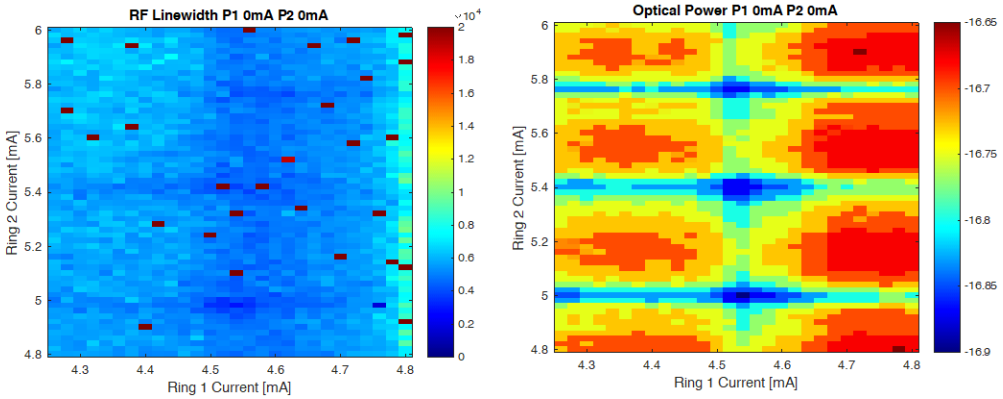

Figure 5.12: RF Linewidth and Optical Power 2D Ring current Scan with phase tuners at 0mA.

Applying current to the phase tuners will result in a direct heating of the whole chip leading to a shift of the rings resonances. We present together RF linewidth and optical power plots to be able to recognize for every current applied where the rings filtering takes place and determine its effect.
For example applying 10mA to both the phase tuners we obtained the following results.

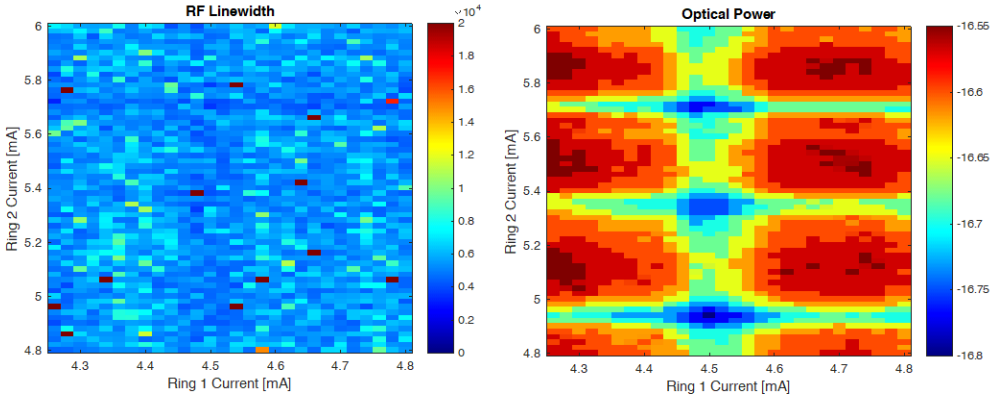

Figure 5.13: RF Linewidth and Optical Power 2D Ring current Scan with phase tuners at 10mA.

We can directly observe, form the optical power, how the resonances shift towards the bottom right corner of the plot and this is consistent since the rings will need less heating current to filter that specific lines, since the phase tuners current is providing additional heating as before. Regarding the linewidth, we can still recognize the feedback effect in terms of linewidth reduction, but the whole effect is weaker and leads to a minimum linewidth between 4 and 5kHz. It's then probable that this phase shift leads to a worse interactions between the input lines and the feedback lines, which are slightly out of phase and won't guarantee a good effect as before.
This is much more evident in the next measurement shown, where, applying 20mA to the phase tuners we can see that the feedback signal is completely out of phase and will lead to a worsening in terms of linewidth.

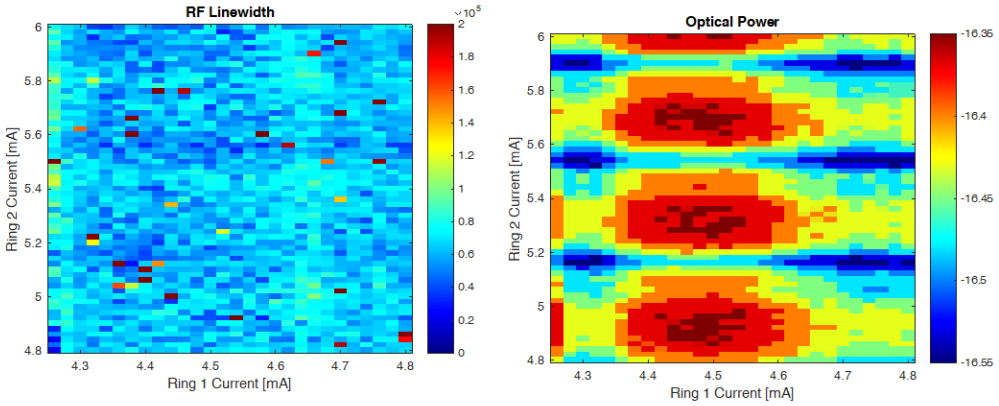

Figure 5.14: RF Linewidth and Optical Power 2D Ring current Scan with phase tuners at 20mA.

Once again, from the optical power, we can see how the resonances move and from the linewidth plot we can clearly observe how the feedback effect is visible but lead to a strong broadening of the RF linewidth with respect to the regions where non line of the comb is filtered by the rings and sent back. This is due to a phase mismatch between the feedback lines and the input signal.

We now apply to the phase tuners a current of 30mA and we obtain the following results.

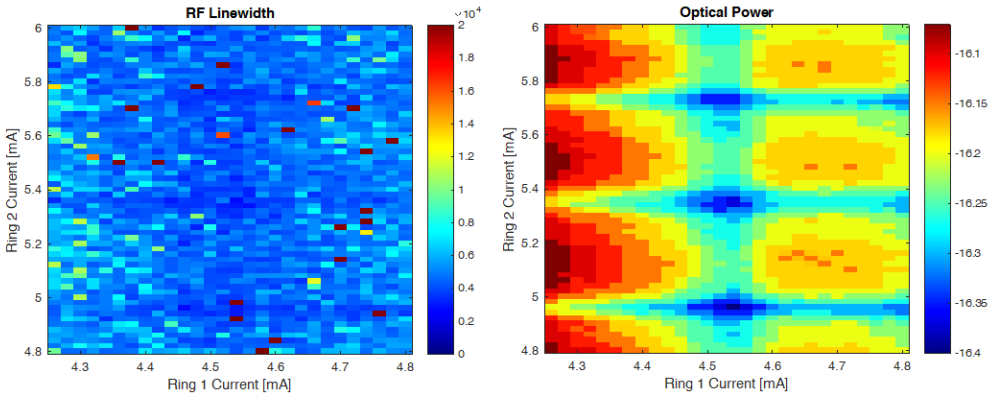

Figure 5.15: RF Linewidth and Optical Power 2D Ring current Scan with phase tuners at 30mA.

We can now see again the beneficial effect of feedback since, in correspondence of the ring resonances, we measured an average linewidth of 3kHz.
In conclusion the tuning of the phase shifters doesn't lead to a significant improvement of the linewidth with respect to the original measurement.

Chapter 6

Conclusions and Outlook for the Future

In this thesis, effects of external tunable optical feedback on a semiconductor mode-locked laser through a photonics integrated circuit were discussed. After a short discussion of laser theory useful for the investigation and external optical feedback theory, the setup and the chip used were presented in detail. We show in chapter 5, through experimental results, how we can reach, tuning the parameters of our external optical feedback, a good and stable locking condition of the laser. This was performed through spatial filtering of single lines of the comb spectrum of the laser with ring resonators. These lines were able to enter the feedback branches, where they experience a phase tuning, and then re-injected in the main branch, where they interact with the laser source. The performances of the laser coupled to the chip are improved, even though not significantly, in terms of RF and optical linewidth, with respect to the free-running condition.

This shows the beneficial effects of tunable external optical feedback on a mode-locked laser and gives good premises for further investigations on the topic. For future research a full four-dimensional scan of all the parameters of the feedback should be implemented, scanning both the rings and the phase shifters continuously.
Also the back-reflections from the chip surface play an important role, since we have a direct coupling, so it would be useful to implement the laser in

a flip-chip configuration on the PIC to avoid this unwanted back-reflections which may cause destructive interference and influence badly our investigation. The system is quite complex, since lots of different effects take place, so it would be extremely useful to decrease the the order of complexity, for example by guaranteeing an higher precision of the rings, making them more selective in order to filter exactly only one line of the comb at a time and reduce as much as possible the back-reflections of every photonic device present in our circuit.

As seen in Chapter 1, state of the art reduction of linewidth was achieved exploiting long delay lines, so it would be really interesting to combine our approach of tunable feedback to a long delay line and investigate the joined effect.

Bibliography

[1] J. Jin, *Dimensional metrology using the optical comb of a mode-locked laser*, Measurement Science and Technology 27, 2016, DOI: 10.1088/0957-0233/27/2/022001

[2] J. Ye, H. Schnatz, L. W. Hollberg, *Optical Frequency Combs: from frequency metrology to optical phase control*, IEEE Journal of selected topics in quantum electronics, Vol. 9, No. 4, July/August 2003

[3] K. Merghem, V. Panapakkam, Q. Gaimard, F. Lelarge, A. Ramdane, *Narrow Linewidth frequency comb source based on self-injected Quantum-Dash passively mode-locked laser*, in Conference on Lasers and Electro-Optics, OSA Technical Digest (online) (Optical Society of America, 2017), paper SW1C.5.

[4] J. Hauck, M. Schrammen, S. Romero-Garcia, J. Müller, B. Shen, J. Richter, F. Merget, J. Witzens, *Stabilization and Frequency control of a DFB laser with Tunable Optical Reflector integrated in a silicon photonics PIC*, Journal of lightwave technology, Vol. 34, No. 23, December 1, 2016

[5] K. Shum, *Density of states in semiconductor nanostructures*, Journal of Applied Physics 69, 6484 (1991); DOI: 10.1063/1.348855

[6] J.P. Reithmaier, G. Eisenstein, A. Forchel, *InAs/InP Quantum-Dash Lasers and Amplifiers*, Proceedings of the IEEE Vol. 95,No. 9, September 2007

[7] J.H. Weik, S. Chan, *A theoretical analysis of quantum dash structures*, Journal of Applied Physics 97, 123524 (2005); DOI: 10.1063/1.1938272

[8] K. Yvind, J.M. Hvam, *Semiconductor Mode-Locked Lasers for Optical Communication Systems*, 2003

[9] H. A. Haus, *A theory of forced mode locking*, IEEE Journal of Quantum Electronics, 11 (7), 323 (1975)

[10] R.G.M.P Koumans, R. van Roijen, *Theory for passive mode-locking in semiconductor laser structures including the effects of self-phase modulation, dispersion and pulse collisions*, IEEE Journal of Quantum Electronics, 1996, DOI: 10.1109/3.485400

[11] M. Young, *Optics and Lasers, Including fibers and optical waveguides*, Springer, 2000

[12] K. Merghem, C. Calo', R. Rosales, X. Lafosse, G. Aubin, A. Martinez, F. Lelarge, *Stability of Optical Frequency Comb generated with InAs/InP Quantum-Dash-Based passive Mode-Locked Lasers*, IEEE journal of quantum electronics, Vol. 50, No. 4, April 2014

[13] S. Donati, R.H. Horng, *The Diagram of Feedback Regimes revisited*, IEEE Journal of selected topics in Quantum Electronics, Vol. 19, No. 4, July/August 2013

[14] E. A. Avrutin, B. M: Russel, *Dynamics and Spectra of Monolithic Mode-Locked Laser Diodes under External Optical Feedback*, IEEE Journal of Quantum Electronics, Vol. 45, No. 11, November 2009

[15] R. Lang, K. Kobayashi, *External Optica Feedback effects on semiconductor injection Laser Properties*, IEEE Journal of Quantum Electronics, Vol. QE-16, No. 3, March 1980

[16] Y. Yu, G. giuliani, S. Donati, *Measurement of the Linewidth Enhancement Factor of semiconductor Lasers based on the Optical Feedback self-mixing effect*, IEEE Photonics Technology Letters, Vol. 16, No. 4, April 2004

[17] T. Habruseva, S. O'Donoghue, N. Rebrova, F. Kefelian, S.P. Hegarty, G. Huyet, *Optical linewidth of a passively mode-locked semiconductor laser*, Optics Letters, Vol. 34, No. 21, November 1, 2009

[18] F. Kefelian, S. O'Donoghue, M.T. Todaro, J.G. McInerney, G. Huyet, *RF Linewidth in Monolithic Passively Mode-Locked Semiconductor Laser*, IEEE photonics technology letters, Vol. 20, No. 16, February 15, 2008

[19] N. Rebrova, G. Huyet, S. P. Hegarty, *Optical linewidth of a passively mode-locked semiconductor laser*, Optics Letters, November 2009, DOI: 10.1364/OL.34.003307

[20] J. Cardenas, C:B. Poitras, K. Luke, L.W. Luo, P. Morton, M. Lipson, *High Coupling Efficiency Etched Facet Tapers in Silicon Waveguides*, IEEE photonics technology letters, doi 10.1109/lpt.2014.2357177

[21] W. Bogaerts, P. De Heyn, T. Van Vaerenbergh, K. De Vos, S.K. Selvaraja, T. Claes, P. Dumon, P. Bienstman, D. Van Thourhout, R. Baets, *Silicon microring resonators*, Laser Photonics Rev. 6, No. 1, 47–73 (2012) DOI: 10.1002/lpor.201100017

[22] I.V. Ermakov *Application of semiconductor lasers with optical feedback*

[23] M.J. Connelly, *Theoretical calculations of the carrier induced refractive index change in tensile-strained InGaAsP for use in 1550 nm semiconductor optical amplifiers*, Applied Physics Letters 93, 181111 (2008)

[24] N.M. Ravindra, P. ganapathy, J. Choi, *Energy gap-refractive index relations in semiconductors*, Infrared Physics and Technology 50 (2007) 21-29

[25] R.M. Waxler, G.W. Cleek, *The EHect of Temperature and Pressure on the Refractive Index of Some Oxide Glasses*, Journal of research of the National Bureau of Standards - A. Physics and Chemistry Vol. 77A, No. 6, November-December 1973

[26] D.B. Mortimore, *Fiber Loop Reflectors*, Journal of lightwave technology, Vol. 6, No 7, July 1988

[27] Y. Fu, T. Ye, W. Tang, T. Chu, *Efficient adiabatic silicon-oninsulator waveguide taper*, Photon Res., Vol. 2, No. 3, June 2014